Bone Histology of Phytosaur, Aetosaur, and Other Archosauriform Osteoderms (Eureptilia, Archosauromorpha)

TORSTEN M. SCHEYER,[1]* JULIA B. DESOJO,[2,3] AND IGNACIO A. CERDA[2,4]
[1]Paläontologisches Institut und Museum der Universität Zürich, Karl Schmid-Strasse 4, CH-8006 Zürich, Switzerland
[2]Consejo Nacional de Investigaciones Científicas y Técnicas (CONICET)
[3]Sección Paleontología Vertebrados, Museo Argentino de Ciencias Naturales "Bernardino Rivadavia", Ángel Gallardo 470 C1405DJR, Buenos Aires, Argentina
[4]Instituto de Investigación en Paleobiología y Geología, Universidad Nacional de Río Negro, Museo Carlos Ameghino, Belgrano 1700, Paraje Pichi Ruca (predio Marabunta), 8300 Cipolletti, Río Negro, Argentina

ABSTRACT

As in other archosauriforms, phytosaurs and aetosaurs are characterized by the presence of well-developed osteoderms. Here we provide a comparative study on the microstructure of phytosaur (five taxa) and aetosaur (thirteen taxa) osteoderms. For outgroup comparison, we sampled osteoderms of the sister taxon to Aetosauria, *Revueltosaurus callenderi*, and the doswelliid *Jaxtasuchus salomoni*. Phytosaur, aetosaur, and *Jaxtasuchus* osteoderms are composed of a diploe structure, whereas the *Revueltosaurus* osteoderm microanatomy is more compact. The external cortex of phytosaurs, *Revueltosaurus* and *Jaxtasuchus* osteoderms is mainly composed of parallel-fibered bone. In aetosaurs, the external cortex mainly consists of lamellar bone, with lines of resorption within the primary bone indicating successive cycles of bone erosion and deposition. The basal cortex in all the specimens is composed of parallel-fibered bone, with the cancellous internal core being more strongly developed in aetosaurs than in phytosaurs. Woven or fibro-lamellar bone was recorded in both phytosaurian and aetosaurian taxa, as well as in *Jaxtasuchus*. Structural fibers, which at least partly suggest metaplastic origin, were only recorded in the internal core of two phytosaurs and in the basal cortex of one aetosaur. Osteoderm thickness and cancellous to compact bone ratios appear to be subject to ontogenetic change. Minimum growth mark counts in osteoderms sampled indicate that some aetosaurs and phytosaurs lived for at least two decades. Bone microstructures are more uniform in phytosaur osteoderms and show a higher level of disparity among aetosaur osteoderms, and at least in the latter, histological features are potentially apomorphic for species/genus level. Anat Rec, 297:240–260, 2014. © 2013 Wiley Periodicals, Inc.

Grant sponsor: Swiss National Science Foundation; Grant number: 31003A_146440.; Grant sponsor: Agencia Nacional de Promoción Científica y Técnica; Grant number: PICT 2012 N° 925.; Grant sponsor: Alexander von Humboldt Foundation.

*Correspondence to: Torsten M. Scheyer, Paläontologisches Institut und Museum der Universität Zürich, Karl Schmid-Strasse 4, CH-8006 Zürich, Switzerland. Fax: +41–44-634-49-23. E-mail: tscheyer@pim.uzh.ch

Received 10 May 2013; Accepted 22 October 2013.
DOI 10.1002/ar.22849
Published online 24 December 2013 in Wiley Online Library (wileyonlinelibrary.com).

Key words: bone microstructure; dermal armor; Phytosauria; Aetosauria; fibro-lamellar bone; archosaurs

INTRODUCTION

Osteoderms (bone mineralizations embedded within the dermis) are widely distributed among different groups of tetrapods (Moss, 1969; Hill, 2005; Sire et al., 2009; Vickaryous and Sire, 2009), such as armadillos, lizards (e.g., the blindworm, some geckos and skinks, etc.) and, in part, the turtle shell. Besides serving as armor or weapons (e.g., Scheyer and Sander, 2004; Hayashi et al., 2012), osteoderms can have various other functions such as calcium-storage in ovipositing female specimens (e.g., in crocodylians: Klein et al., 2009 and references therein), stabilization of the vertebral column (e.g., Frey, 1988; Buchwitz et al., 2012), and heat-regulation and/or species recognition (discussed in Farlow et al., 2010 and Hayashi et al., 2012). In archosauriforms, these elements are a prominent part of the skeleton, including pseudosuchian (the lineage leading to modern crocodylians) and avemetatarsalian representatives, and are often of systematic value (e.g., Nesbitt, 2011). Within non-avemetatarsalian archosauriform lineages, Phytosauria and Aetosauria are two osteoderm bearing clades of particular interest, as they represent the two clades with most complete sets of dorsal, ventral (gular shield in phytosaur), and appendicular osteoderms known.

Phytosaurs resemble modern long-snouted crocodylians in outer body shape and probably semi-aquatic lifestyle, but their external nostrils are positioned close to the eyes and not at the tip of the rostrum (e.g., Gregory, 1962; Romer, 1966; Chatterjee, 1978; Hunt, 1989a; Hungerbühler, 2002; Stocker and Butler, 2013). Phytosauria are considered by most researchers to be restricted to the Upper Triassic, although some earlier phytosaur remains were described also from the Lower Triassic (Buntsandstein, material lost during World War II) of Germany (Jaekel, 1910; Buffetaut, 1993)—neither the systematic position of that specimen nor its age estimation are certain however. A similar situation exists for the youngest phytosaur record from the Blue Lias Formation of Somerset, UK (Hillebrand and Krystyn, 2009). Phytosaurs (also sometimes referred to as parasuchians) were often recovered in a monophyletic Pseudosuchia together with "rauisuchians", ornithosuchids, aetosaurs, and crocodylomorphs, the lineage leading to crown-clade Crocodylia (e.g., Brusatte et al., 2010); however they were recently suggested to lie outside of Pseudosuchia (Fig. 1), constituting the sister group to Archosauria instead (Nesbitt, 2011; Stocker and Butler, 2013).

Aetosauria constitute another prominent group of armored, quadrupedal archosaurs from the Upper Triassic time period, which were widespread over South America, North America, Greenland, Europe, North Africa, ?Madagascar, and the Indian subcontinent (Heckert and Lucas, 2000; Parker, 2007; Desojo and Ezcurra, 2011; Desojo et al., 2013). Aetosaur osteoderm morphology has often been used to diagnose taxa and to utilize aetosaurs as index fossils for biochronological correlations of Upper Triassic strata-level (e.g., Long and Ballew, 1985; Heckert and Lucas, 2000). However, there are limitations of this osteoderm determination, because several taxa possess similar ornamentation patterns of the paramedian osteoderms (e.g., *Aetosauroides*, *Aetosaurus*, *Calyptosuchus*, *Neoaetosauroides*, *Stagonolepis*), and there is significant morphological variation of homologous osteoderms within and among aetosaur taxa (Parker, 2007; Parker and Martz, 2010).

A previous study on "rauisuchian" osteoderm histology (Scheyer and Desojo, 2011) used a set of four archosauriform osteoderms for outgroup comparison. Therein, the few aetosaur and phytosaur osteoderms used were reported to "generally show parallel-fibered or lamellar-zonal bone tissue" (Scheyer and Desojo, 2011: p. 1296), whereas slightly raised growth rates, based on the presence of fibro-lamellar bone, were indicated for "rauisuchian" osteoderms (see also Cerda et al., 2013). Otherwise, comparatively little has been published on aetosaur and phytosaur osteoderm histology (e.g., Heckert and Lucas, 2002; Scheyer and Sander, 2004; Parker et al., 2008; Cerda and Desojo, 2011). This is rather surprising, given the number of identifiable osteoderms recovered in the field (as they are more common than long bone material in some cases, such as the aetosaur osteoderms recovered in the Late Triassic outcrops of North America), as well as their taxonomic value.

To elucidate the morphogenesis and growth rates of these taxonomically important skeletal elements within Archosauriformes, we here report on the bone microstructures of a broader sample of aetosaurian (thirteen taxa) and phytosaurian (five taxa) osteoderms, as well as on osteoderms of *Revueltosaurus* and the recently described doswelliid non-archosaurian archosauriform *Jaxtasuchus* from Germany (Schoch and Sues, 2013).

MATERIALS AND METHODS

In this study, various paramedian osteoderms or osteoderm fragments of archosauriforms (Fig. 1) were sampled and all material sampled in the present study is compiled in Table 1. If not explicitly stated otherwise, the position of the osteoderm on the body of the animal is unknown.

The phytosaur sample (Fig. 2) of the present study included osteoderms of *Leptosuchus*, *Paleorhinus*, *Pseudopalatus*, and Phytosauria (all North America), as well as Phytosauria from Germany. Another previously sampled and described appendicular osteoderm (Stocker and Butler, 2013) identifiable only as belonging to Phytosauria is also included in the discussion (Scheyer and Sander, 2004). Although phytosaur osteoderms are currently not considered to be species-diagnostic (Michelle Stocker, personal communication 2012), the specimens

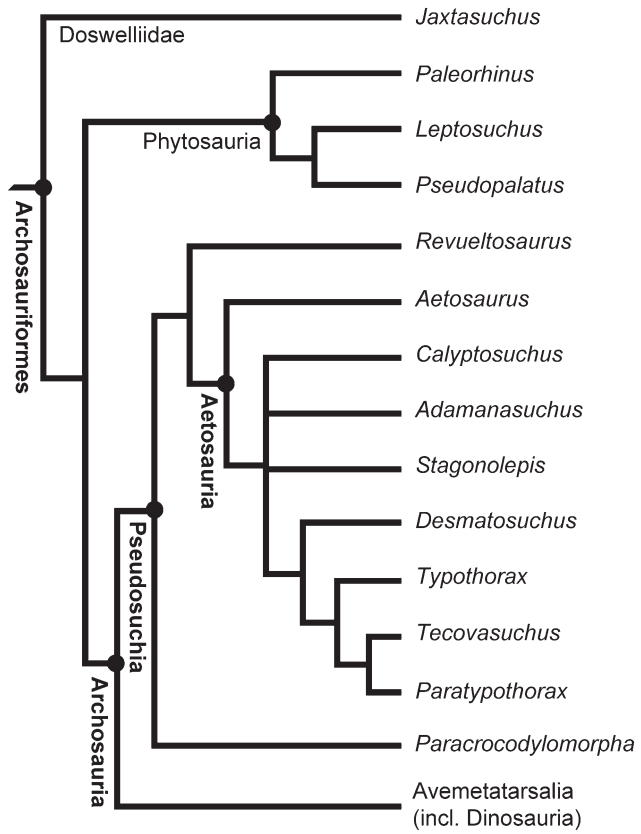

Fig. 1. Working framework showing the genera included in the present study. The composite hypothetical relationships are based on Desojo et al. (2012), Nesbitt (2011), and Stocker (2012).

used in the study were found together or at least closely associated with skull material, which warrants a specific identification. In case of specimen TTU-P14639-t referred to *Leptosuchus*, the osteoderm was found ca. 4 m apart from a *Leptosuchus* skull in the same layer, and all other identifiable fragments from the locality belong to *Leptosuchus* as well. TTU-P11554 was found 3–4 m apart from a *Pseudopalatus* skull in the same layer, and no other phytosaur has been recognized in that locality. In the case of specimen TTU-P19255 from the Dockum Group, the osteoderm was originally referred to *Angistorhinus* sp. Because it was not directly associated to diagnostic skull material, and because *Paleorhinus* might also occur in the same locality (Bill Mueller, personal communication 2012), we conservatory refer it to Phytosauria.

Phytosauria itself was repeatedly recovered as a monophyletic clade (e.g., Ballew, 1989; Parker and Irmis, 2006; Brusatte et al., 2010; Stocker 2010, 2012; Nesbitt, 2011). Based on Stocker (2012) as main reference, our sampling thus covers basally positioned Phytosauria (*Paleorhinus*), as well as a more highly nested member of pseudopalatine Leptosuchomorpha (*Pseudopalatus*).

The aetosaur (Fig. 3) sample included osteoderms of *Aetosaurus ferratus* and *Paratypothorax andressorum* (Germany), *Stagonolepis olenkae* (Poland), and *Adamanasuchus eisenhardtae*, *Calyptosuchus wellesi*, *Desmatosuchus smalli*, and *D. spurensis*, *Paratypothorax*, Stagonolepididae unnamed species, *Tecovasuchus chatterjeei*, and *Typothorax* (all North America). Due to their taxonomic utility, it was possible to confidently identify aetosaur taxa based on isolated osteoderms even if they were not associated with other skeletal material. Using the phylogenetic analysis of Desojo et al. (2012) as a framework, the sampling of osteoderms thus encompasses both major lineages within stagonolepidid aetosaurs, the Typothoracisinae (*Paratypothorax*, *Tecovasuchus*, *Typothorax*), and the Desmatosuchinae (*Desmatosuchus*), as well as approximate outgroups to stagonolepidids (*Aetosaurus*, *Calyptosuchus*, *Stagonolepis*). *Adamanasuchus eisenhardtae* as described by Lucas et al. (2007) was not included in Desojo et al.'s (2012) analysis or in any other recent taxonomic study, and so its position among aetosaurs remains unresolved so far. *A. eisenhardtae* was nonetheless included in the present study to elucidate whether the features of a "distinctive dorsal armor that present a unique mosaic of characteristics seen individually in other aetosaur genera" (Lucas et al., 2007: p. 246) can also be recognized on the histological level.

A preliminary report on the osteoderm microstucture of the non-aetosaurian pseudosuchian *Revueltosaurus callenderi* from the Upper Triassic Chinle Formation, Petrified Forest National Park, Arizona (Parker et al., 2005, Nesbitt, 2011) was given in Scheyer and Desojo (2011). Here, the histological data of *Revueltosaurus* are described in detail and used to elucidate the morphogenesis and structure among the aetosaur osteoderms sampled. Furthermore, two osteoderms (Fig. 3I,J) of the new doswelliid archosauriform *Jaxtasuchus* (Schoch and Sues, 2013) were sectioned for outgroup comparison.

Following standard petrographic thin-sectioning procedures (e.g., Chinsamy and Raath, 1992, Chinsamy-Turan, 2005; Lamm, 2013) all osteoderms were sectioned either longitudinally or transversely to allow comparability among taxa. Prior to sectioning with a stone saw equipped with a diamond-sintered blade, the specimens were embedded in a two-component synthetic resin (Araldit XW396 and XW397). The same resin was then used for stabilization and filling of holes and fixing of the specimens to glass slides. After cutting the specimen off the slide (again using the stone saw), the remaining bones on the slide were ground down to a thickness of 60–80 μm or less (depending on the natural coloration of the bones), using SiC powders (usually SiC 500, SiC, 800).The samples were then covered with a thin glass cover slip using UV-resin (Panacol Vitralit 6127) and a UV handlamb (UVAHAND 8/BL). The specimens were then studied with a LEICA compound microscope DM 2500 M equipped with a LEICA digital camera DFC 420C. In the case of *Revueltosaurus*, polished sections (using SiC 1200 polishing powder) were prepared in addition to the thin sections, to be studied under reflected light conditions. Nomenclature of osteoderm structures is following Cerda and Desojo (2011). As such the terms "external," "internal" (for core area of osteoderm), and "basal" are used herein (which correspond, respectively, to "external," "interior," and "internal" of Scheyer and Desojo, 2011). All sections will be returned to and kept with the reminder of the bone specimens in the specific institutions and collections.

Institutional Abbreviations: PEFO, Petrified Forest National Park, Arizona, USA; SMNS, Staatliches

TABLE 1. Taxon names, specimen numbers, and locality data of archosauriform specimens

Taxon sampled	Specimen no.	Age and locality information
Phytosauria		
Leptosuchus	TTU-P14639-t (keeled osteoderm fragment)	lower Tecovas Formation, Dockum Group, Upper Triassic, Crosby County, Texas
Paleorhinus	TTU-P18243 (keeled osteoderm fragment associated with TTU-P09423, a complete skull and partial postcranium)	lower Tecovas Formation, Dockum Group, Upper Triassic, Garza County, Texas
Pseudopalatus	TTU-P11554 (osteoderm fragment)	upper Cooper Canyon Formation, Dockum Group, Norian, Upper Triassic, Garza County, Texas
Phytosauria	TTU-P19255 (keeled osteoderm fragment, originally referred to as *Angistorhinus* sp.)	middle Tecovas Formation, Dockum Group, Carnian, Upper Triassic, Borden County, Texas
Phytosauria	IPB R479 (small, roughly circular osteoderm with central apex; see Scheyer and Sander, 2004)	Cooper Canyon Formation, Dockum Group, ?Norian, Upper Triassic, Garza County, Texas
Phytosauria	SMNS 91013 (keeled osteoderm fragment; previously identified as cf. *Mystriosuchus* sp.)	Löwenstein Formation, Norian, Upper Triassic, Heslach near Stuttgart, Germany
Aetosauria		
Adamanasuchus eisenhardtae Lucas et al., 2007	TTU-P10593 (paramedian osteoderm fragment)	lower Tecovas Formation, Dockum Group, Upper Triassic, Crosby County, Texas
Aetosaurus ferratus Fraas, 1877	SMNS 12670 (thin paramedian osteoderm fragment of *Aetosaurus ferratus* specimen, see Schoch, 2007)	Arnstadt Formation (middle Stubensandstein), Norian, Upper Triassic, Pfaffenhofen, southern Germany
Calyptosuchus wellesi (Long and Ballew, 1985)	PEFO 34191 (paramedian osteoderm fragment; listed also in Parker and Martz, 2011: Table 1 as part of the voucher specimens used in stratigraphic range chart reconstruction)	upper Lots Wife beds, Sonsela Member, Chinle Formation, Norian, Petrified Forest National Park, Arizona
Desmatosuchus smalli Parker, 2005	TTU-P09204-z (paramedian osteoderm fragment associated with postcranial material)	top of Tecovas Formation, Dockum Group, Carnian, Upper Triassic, Garza County, Texas
Desmatosuchus spurensis Case, 1920	TTU-P16092-v (isolated cervical lateral osteoderm based on external surface ornamentation; see Parker, 2005)	lower Tecovas Formation, Dockum Group, Upper Triassic, Crosby County, Texas
Paratypothorax andressorum Long and Ballew, 1985	SMNS 91551 (paramedian osteoderm fragment associated with other skeletal remains)	Löwenstein Formation (Stubensandstein), Norian, Upper Triassic,from type locality Heslach near Stuttgart, Germany
Paratypothorax sp. (*Paratypothorax* Long and Ballew, 1985)	PEFO 5030 (larger paramedian osteoderm fragment)	above Lithodendron Wash bed, Petrified Forest Member, Chinle Formation, upper Norian, Petrified Forest National Park, Arizona
	PEFO 34187 (small paramedian osteoderm fragment)	top of Jim Camp Wash beds, Sonsela Member, Chinle Formation, Norian, Petrified Forest National Park, Arizona
	TTU-P11594 (paramedian osteoderm fragment, originally referred to as *Calyptosuchus wellesi*)	lower Tecovas Formation, Dockum Group, Upper Triassic, Crosby County, Texas
Stagonolepis olenkae Sulej, 2010	ZPAL Ab III/2379 (four paramedian osteoderm fragments, two of which were sampled herein)	probably Drawno Beds coeval to the Lehrberg Beds of Germany, Late Carnian, Upper Triassic, Krasiejów, Opole Silesia, southern Poland
Stagonolepididae unnamed sp.	TTU-P18443-b (small thick osteoderm fragment, associated with most of the carapace)	near base of Cooper Canyon Formation, Dockum Group, Norian, Upper Triassic, Garza County, Texas
Tecovasuchus chatterjeei Martz and Small, 2006	TTU-P19902 (paramedian osteoderm fragment)	lower Tecovas Formation, Dockum Group, Upper Triassic, Crosby County, Texas

TABLE 1. (continued).

Taxon sampled	Specimen no.	Age and locality information
Typothorax Cope, 1875	PEFO 5039 (smaller paramedian osteoderm fragment, originally identified as *Typothorax* cf. *T. coccinarum*)	top of Jim Camp Wash beds, Sonsela Member, Chinle Formation, Norian, Petrified Forest National Park, Arizona
	PEFO 36853 (larger paramedian osteoderm fragment)	exact locality unknown, upper part of Sonsela Member, Chinle Formation, Norian, Petrified Forest National Park, Arizona
	SMNS 91550 (isolated paramedian osteoderm fragment)	Santa Rosa Formation (Santa Rosa Sandstone?), Chinle Group, Carnian, Conchas Lake, New Mexico
Non-aetosaurian Pseudosuchia		
Revueltosaurus callenderi Hunt, 1989 (Hunt, 1989b)	PEFO 35283 (small paramedian osteoderm; see Scheyer and Desojo, 2011)	Chinle Formation, Upper Triassic, Petrified Forest National Park, Arizona
Non-archosaurian Archosauriformes		
Jaxtasuchus salomoni Schoch and Sues, 2013	SMNS 81902 (larger osteoderm fragment); SMNS 91549 (smaller osteoderm fragment)	Erfurt Formation (Lower Keuper), late Ladinian, late Middle Triassic, Schumann Quarry, Vellberg (Eschenau), east of Schwäbisch Hall, Baden-Württemberg, Germany

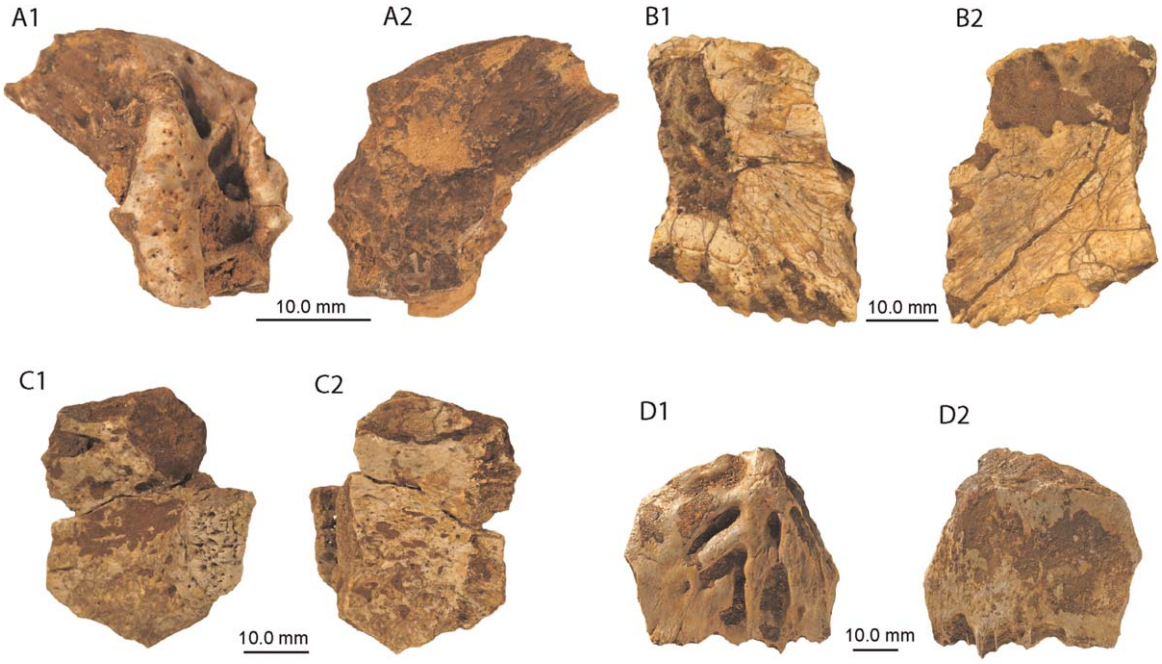

Fig. 2. Sampled phytosaur osteoderms. **A**: *Leptosuchus* (TTU-P14639-t). **B**: *Pseudopalatus* (TTU-P11554). **C**: *Paleorhinus* (TTU-P18243). **D**: Phytosauria (TTU-P19255). Images marked with 1 in external and with 2 in basal view. Specimens are arranged so that keel/long axis is antero-posteriorly orientated.

Museum für Naturkunde, Stuttgart, Germany; TTU, Museum of Texas Tech University, Lubbock, Texas, USA; ZPAL, Institute of Palaeobiology of the Polish Academy of Sciences, Warsaw, Poland.

RESULTS

Phytosauria

All phytosaur osteoderms have a diploe structure with a variably developed extensive internal core area, surrounded by external and basal compact bone. The external osteoderm surface is strongly sculptured, especially in the central keeled regions, whereas the basal bone surface is usually flat to slightly concave. Only in the Phytosauria specimen IPB R479 (Scheyer and Sander, 2004), which most likely is a non-median appendicular osteoderm, the basal surface is convex. These differences might pertain to the osteoderm position on the body (anterior-posterior or medial-lateral). In all specimens, the cortices are well vascularized and roughly of similar thickness.

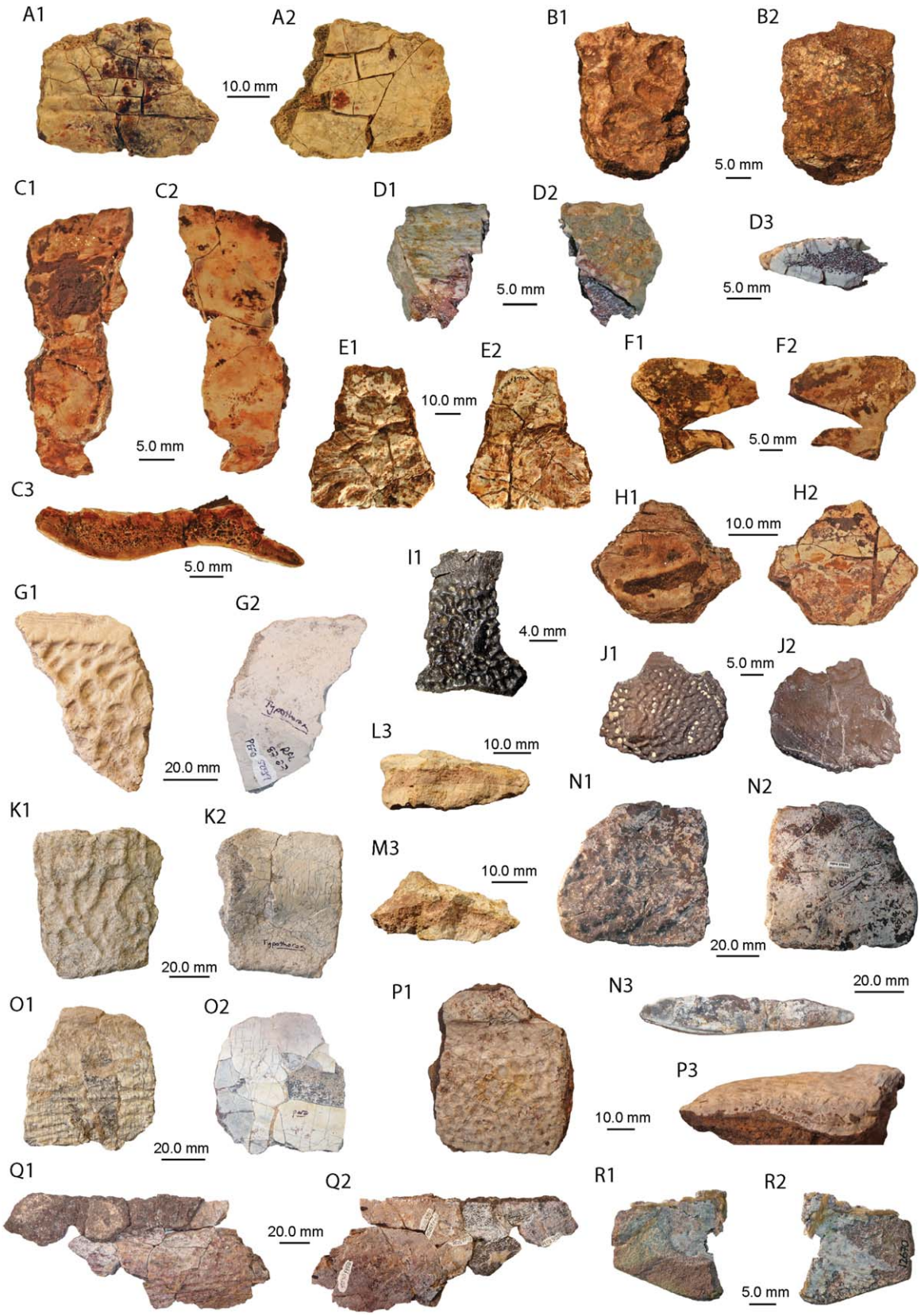

Fig. 3. Sampled aetosaur and outgroup osteoderms. **A**: *Paratypothorax* (TTU-P11594). **B**: *Desmatosuchus spurensis* (TTU-P16092-v). **C**: *Tecovasuchus chatterjeei* (TTU-P19902). **D**: *Paratypothorax andressorum* (SMNS 91551). **E**: *Desmatosuchus smalli* (TTU-P09204-z). **F**: *Adamanasuchus eisenhardtae* (TTU-P10593). **G**: *Typothorax* (PEFO 5039). **H**: Stagonolepididae unnamed sp. (TTU-P18443-b). **I**: *Jaxtasuchus salomoni* (SMNS 91549). **J**: *Jaxtasuchus salomoni* (SMNS 81902). **K**: *Typothorax* sp. (PEFO 36853). **L**, **M**: *Stagonolepis olenkae* (ZPAL Ab III/2379). **N**: *Calyptosuchus wellesi* (PEFO 34191). **O**: *Paratypothorax* (PEFO 34187). **P**: *Typothorax* (SMNS 91550). **Q**: *Paratypothorax* (PEFO 5030). **R**: *Aetosaurus ferratus* (SMNS 12670). Images marked with 1 in external, with 2 in basal, and with 3 in lateral view. If possible, specimens are arranged with their anterior margin facing to the top of the figure.

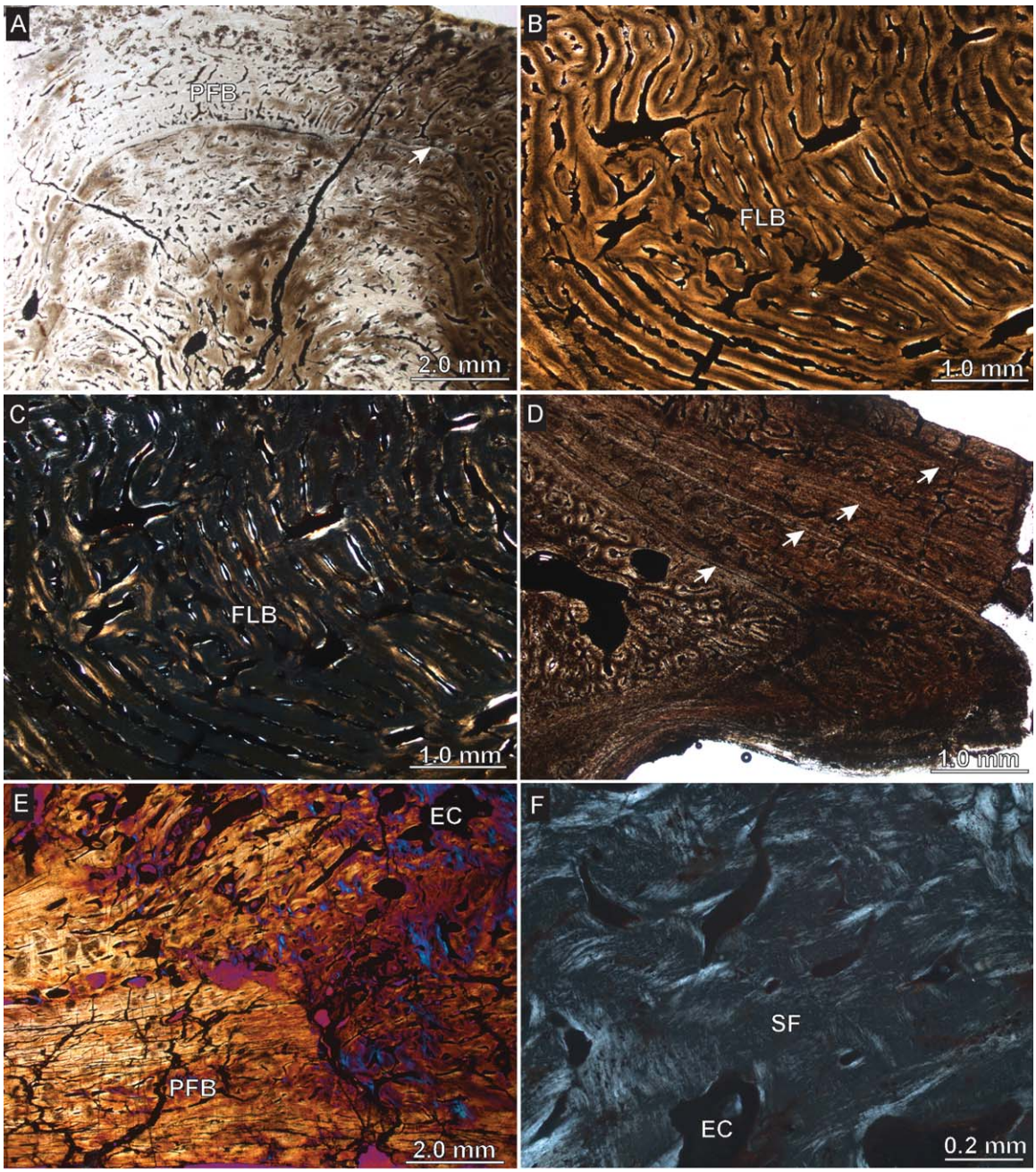

Fig. 4. Phytosaur osteoderm histology, part I. **A–C**: Phytosauria (TTU-P19255). **D**: *Leptosuchus* (TTU-P14639-t). **E**,**F**: Phytosauria (SMNS 91013). Images in A, B and D are shown in normal polarized transmitted light, C and F in cross-polarized light and E in cross-polarized light using a lambda compensator. A: External cortex over keeled area of osteoderm. A growth mark (Line of arrested growth) is marked by white arrow. B,C: Localized fibro-lamellar organization (plexiform arrangement of primary osteons) of external bone cortex. D: Cortical bone showing four growth cycles (succession of growth zones, annuli and lines of arrested growth, the latter marked by white arrows) surrounding the internal osteoderm core. E: Dense internal core area of osteoderm surrounded by external and basal cortical bone. In both cortices, layers with higher vascularization intercalate with those with low vascularization. F: Internal core area of osteoderm showing interwoven patterns of structural fibers. Abbreviations: EC, erosion cavity; FLB, fibro-lamellar bone; PFB, parallel-fibered bone; SF, structural fibers.

Phytosauria (TTU-P19255, keeled osteoderm fragment). The cortices are of similar thickness in the specimen. Eight growth marks, that is, annuli, could be traced within the whole compact bone.

External cortex—The cortex consists mainly of a cyclical succession of growth zones (Fig. 4A), usually of parallel-fibered bone extensively vascularized by a reticular network of simple primary vascular canals and

primary osteons, and avascular annuli of parallel-fibered bone. Locally, however, portions of bone appear to be of the fibro-lamellar type (isotropic matrix and vascular canals seamed with lamellar bone in cross-polarized light), with the vascularization reaching plexiform organization (Fig. 4B,C). Sharpey's fibers extend into the cortex in high to moderate angles (about 40° to 70°) and are most conspicuous as coarse fibers in the keeled parts of the osteoderm.

Cancellous bone—The cancellous bone is composed of thick trabeculae preserving interstitial primary bone and vascular spaces lined with lamellar bone. The transition from the core area to the surrounding cortex is distinct, because there is no transitional zone dominated by secondary osteons or erosion cavities.

Basal cortex—The cortex consists of parallel-fibered bone, which is vascularized by a network of primary vascular canals and primary osteons. A single large vascular space of circular shape is present in the cortex, which is interpreted as a large nutrient foramen pervading the osteoderm. Sharpey's fibers are also present within the basal cortex, although they are not as conspicuous as in the external cortex.

Leptosuchus *(TTU-P14639-t, keeled osteoderm fragment).* Previous growth stages of the osteoderm are clearly observable and not remodeled, which allowed a confident count of growth cycles, which showed annuli and LAGs in the sample. Throughout the osteoderm, four growth cycles were counted (Fig. 4D).

External cortex—The external cortex constitutes growth cycles of strongly vascularized zones of parallel-fibered bone tissue interspersed by less vascularized annuli of the same matrix. Sharpey's fibers that insert perpendicularly or in high angles (>60°) into the cortex are abundant.

Cancellous bone—The core area consists of primary bone matrix and vascular cavities. The largest cavities are situated in the center, whereas towards the cortices, smaller vascular spaces and scattered secondary osteons are found.

Basal cortex—The cortex also consists of cyclically deposited parallel-fibered bone, with the growth zones being vascularized by reticular network of vascular canals. Here the growth marks, that is, LAGs, are most conspicuous. Primary osteons or patches of fibro-lamellar bone were not encountered. Sharpey's fibers also insert into the basal cortical bone.

Phytosauria (SMNS 91013, keeled osteoderm fragment, previously identified as cf.* Mystriosuchus *sp.). The earlier identification of the specimen as cf. *Mystriosuchus* sp. is doubtful, as *Mystriosuchus* is not known from the Stuttgart-Heslach locality (identifiable cranial material belongs to *Nicrosaurus* instead: Hungerbühler, 2002). The cortices in this specimen are of similar thickness, but growth marks are not traceable.

External and basal cortices—Both cortices are composed of incremental layers of stronger and less strongly vascularized parallel-fibered bone tissue (Fig. 4E). Fine Sharpey's fibers are found inserting the tissue in the external keel areas, whereas more coarse bundles of Sharpey's fibers extend into the basal cortex. All fibers are slightly angled (between 50° and 80°) towards the core area deep to the osteoderm keel. In both cortices, vascularization consists of a reticular arrangement of primary vascular canals.

Cancellous bone—The cancellous core is most extensive deep to the keel and it tapers off in thickness towards the flatter osteoderm margins. In the internal core area, larger vascular spaces are irregular shaped and smaller spaces are more round. In between the spaces, interstitial primary bone tissue, in patches showing an interwoven pattern of structural fibers, is preserved (Fig. 4F). True trabecular bone is absent in the specimen.

Paleorhinus *(TTU-P18243, keeled osteoderm fragment).* The cortices are of similar thickness, except in the keel, where the internal cancellous core extends partly up to the external bone surface. There is no indication that extensive erosion of the external cortex led to the exposure of the core tissue here, but instead it appears to be a genuine histological feature of the osteoderm. A similar pattern has been recently described in an osteoderm from the caudal region of the South American "rauisuchian" *Fasolasuchus tenax* (Cerda et al., 2013).

External cortex—The external cortex is composed of parallel-fibered bone, vascularized by simple primary canals and primary osteons. Locally, highly vascularized patches of tissue (almost like patches of trabecular tissue) can be found intercalated with the less vascularized layers in the keeled area. Much of the cortex is in the process of being remodeled as evidenced by the presence of scattered secondary osteons throughout the deeper cortical layers (Fig. 5A). At least six growth marks, LAGs and annuli, are traceable within the compact bone, but the remodeling does not allow for getting reliable counts.

Cancellous bone—The internal core shows a complex structure of smaller secondary osteons, several generations of larger erosion cavities, which range from being newly formed to be completely lined with secondary lamellar bone, and small patches of interstitial primary bone. The latter consists of interwoven structural fibers.

Basal cortex—The basal cortex appears bi-partite in structure. The deeper part bordering the internal cancellous core is composed of lamellar-zonal bone sparsely vascularized by scattered primary vascular canals (Fig. 5B,C). Coarse bundles of Sharpey's fibers extending perpendicularly to the basal osteoderm surface are found throughout this part. The more superficial part of the cortex lacks to a large degree the lamellar-zonal organization but consists of a thick zone of parallel-fibered bone heavily crossed by diagonally arranged coarse bundles of Sharpey's fibers. Only a thin band of bone directly adjacent to the basal osteoderm surface again shows a more highly ordered organization, that is, lamellar-zonal bone. The basal osteoderm surface itself is slightly irregular as evidenced by small bony protrusions and excavations formed by this outermost thin band of cortical bone.

Pseudopalatus *(TTU-P11554, osteoderm fragment).* In this specimen, a keel was not encountered, leaving both the external bone surface slightly convex

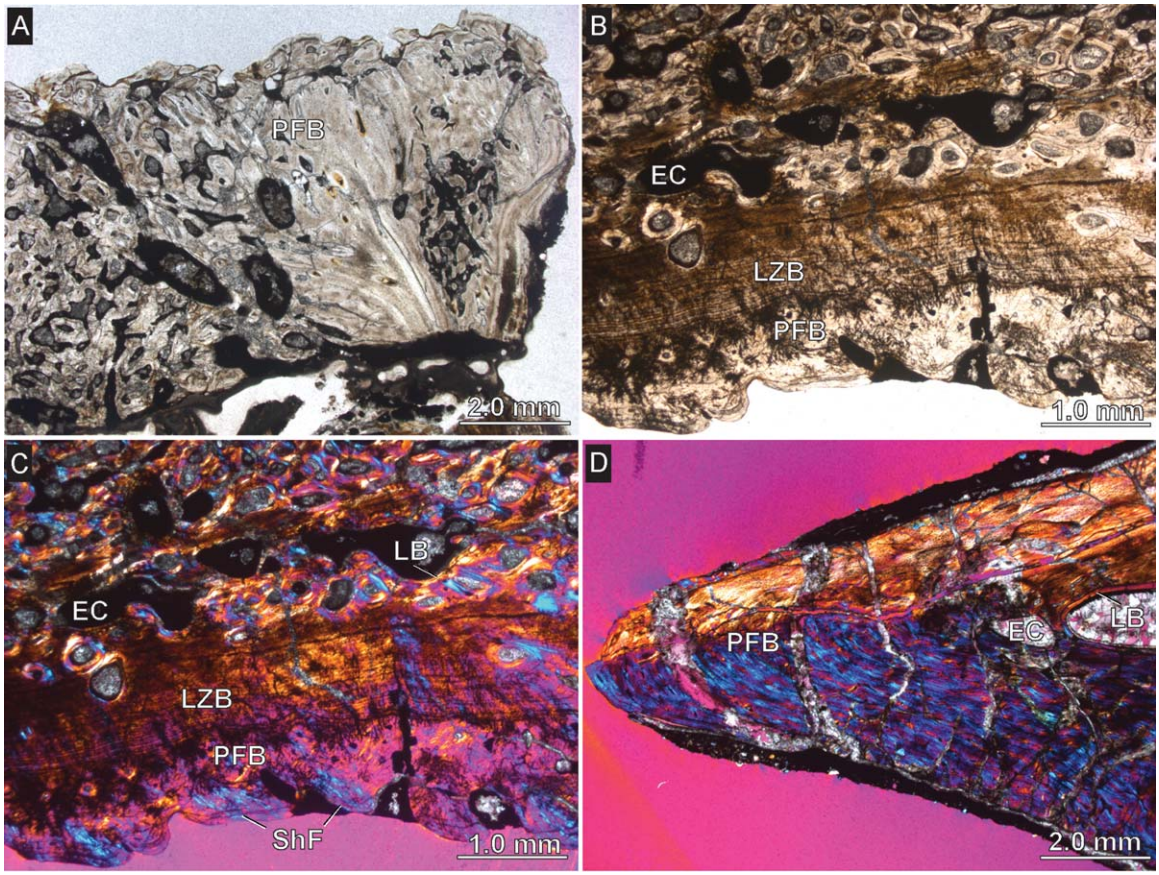

Fig. 5. Phytosaur osteoderm histology, part II. **A–C**: *Paleorhinus* (TTU-P18243). **D**: *Pseudopalatus* (TTU-P11554). Images in A and B are shown in normal polarized transmitted light, C and D in cross-polarized light using a lambda compensator. A: External cortex of keeled area of osteoderm. Note vascularization reaching up to the bone surface. B,C: Interior core area and bipartite basal cortex. Note transition between lamellar-zonal and parallel-fibered bone tissues. D: External and basal cortices of osteoderm. Note how fibrous scaffold changes direction (indicated by change from blue to yellow colors). Abbreviations: EC, erosion cavity; LB, lamellar bone; LZB, lamellar-zonal bone; PFB, parallel-fibered bone; ShF, Sharpey's fibers.

and the basal surface slightly concave. The basal cortex is also thicker than the external cortex surrounding a well-defined internal core area.

External and basal cortices—Both cortices are composed of a homogenous zone of parallel-fibered bone, vascularized by a reticular meshwork of primary vascular canals. At the upturned tapering osteoderm margin, the intrinsic fibers of the compact bone tissue are changing their orientation to continue running parallel to the osteoderm surface (Fig. 5D). In the opposite downturned taping margin, this flexure of the tissue is less obvious, because the bone tissue has a more fibrous texture here (maybe due a higher amount or coarse Sharpey's fibers in this area). Fine Sharpey's fibers extend into the external cortical tissue, whereas coarser Sharpey's fiber bundles extend into the basal cortex. Basally, the coarse bundles are overall angled (between 20° and 60°) towards the internal center of the core area. There is only a single growth mark, an annulus separating the osteoderm core from the cortical bone, identifiable.

Cancellous bone—The cancellous core consists of mostly larger, irregularly shaped vascular spaces lined with secondary lamellar endosteal bone and a few thick trabeculae preserving primary bone internally. Due to the high amount of re-crystallization of the internal core area, the nature of the primary tissue is obscured. A patch of Haversian bone is encountered at the border of the core to the external cortex. Such a transition is not visible towards the basal cortex. Here the border between core area and cortex is highly distinct.

Aetosauria

All sectioned aetosaur osteoderms revealed a well-developed diploe structure with external and basal compact bone layers framing an internal cancellous bone core. Changes in thickness within the cortices are linked to areas of strong bone remodeling only. Depending on the overall thickness of the sampled bone, the core area (internal region) of the osteoderms could be quite extensive. Some of the specimens share histological features, so they have been combined in the descriptive parts below.

Adamanasuchus eisenhardtae *(TTU-P10593, small paramedian osteoderm fragment)*. The sampled fragment is part of several osteoderms in the TTU collections, which resemble the morphology of

Adamanasuchus eisenhardtae described by Lucas et al. (2007), who noted that the paramedian osteoderms are strongly arched (about 30°) and relatively narrow, with prominent anterior bar and ventral keel, and ornamentation with little radiation and sparse circular pits. Unfortunately, due to its fragmentary nature, most of the above characteristics (besides the prominent bar) are indiscernible in the fragment used and only allow us to refer it to Aetosauria.

External and basal cortices—The compact bone layers consist basically of parallel-fibered bone vascularized by scattered simple primary vascular canals (Fig. 6A). Towards the interior core area of the osteoderm, the vascularization gets more extensive with the canals showing reticular patterns. Locally the outermost layers of the external cortex consist of lamellar-zonal bone. Locally, towards the anterior tapering tip of the specimen, four growth cycles are counted (Fig. 6A).

Cancellous bone—A larger area of trabecular bone is present only in the interior-most and thickest part of the osteoderm (Fig. 6A). Here the trabeculae consist of thick secondary lamellar bone. In the other areas, the bone matrix still consists of parallel-fibered tissue but trabeculae are absent and an extensive reticular network of thick primary vascular canals and primary osteons is present instead (Fig. 6B).

Aetosaurus ferratus *(SMNS 12670, small thin fragment)*. Diploe structure—The cortices are thin bands of lamellar bone surrounding an internal core area (Fig. 6C). One compact layer (presumably the external cortex, based on comparison with the other samples) has an increased extensive vascularization system consisting of thick primary vascular canals. No growth marks are visible in the cortical bone. In the two-dimensional section, the trabeculae appear as wide-spaced "floating isolated islands" of bone and trabecular branching points are few and scattered in the section. Otherwise, the specimen lacks diagnosable histological features.

Calyptosuchus wellesi *(PEFO 34191, paramedian osteoderm fragment)*. External cortex—The cortex consists of lamellar-zonal bone, which shows a high degree of remodeling. Lines of resorption are frequently found in the tissue and many intersections occur between successively deposited layers (Fig. 6D). Fine Sharpey's fibers insert into the cortex in high angles (>60°). Thicker areas below ornamental saddles show a generally isotropic fibrous tissue structure with reticular vascularization patterns and rounded osteocyte lacunae. These properties indicate the localized presence of woven fibered bone. A minimum of seven growth cycles (growth zones and LAGs) were counted.

Cancellous bone—The trabecular bone is secondary in nature, constituting centripetally deposited lamellar bone.

Basal cortex—There is a clear thin border between the internal core and the basal cortex. Adjacent to the internal core, the cortex is dominated by a loose arrangement of intercalated longitudinally and transversely extending structural fiber bundles. The latter have a lenticular shape in cross-section. Towards the basal bone surface, the amount of layers with a parallel-fibered texture increases and finally the whole tissue is composed of parallel-fibered bone tissue (Fig. 6E,F). Conspicuous Sharpey's fibers are restricted to the parallel-fibered tissue and are not found in the more internal part of the cortex. Both the inner and outer parts of the cortex are vascularized by scattered simple or branching primary vascular canals and primary osteons.

Isolated pockets of convoluted, well-vascularized secondary bone (Fig. 6E) within the primary bone might be the result of a highly localized pathology (maybe lesion caused by osteitis/osteomyelitis within parts of the basal cortex; see Rothschild et al., 2012 for causes and discussion). Another explanation of these peculiar isolated occurrences of secondary bone might be that they are the result of localized resorption domains caused by increased calcium mobilization (e.g., in ovipositing females). Counting growth marks is largely hampered by delamination of cortical layers.

Desmatosuchus smalli *(TTU-P09204-z)* and Desmatosuchus spurensis *(TTU-P16092-v)*. Both specimens sampled show a strong surface relief (see Parker, 2005), which is also visible as ornamental valleys and saddles in the sections.

External cortex—The external cortex is composed of lamellar bone locally grading into parallel-fibered bone (Fig. 7A). Zonation of the tissue is clearly observable, with five to six growth cycles being present in both specimens (*D. smalli* and *D. spurensis*, respectively). The vascularization of the compact tissue is overall low, consisting only of scattered secondary osteons and erosion cavities. Most of the interior compact layers on the other hand are heavily remodeled, so that there is no distinct transitional zone between the external cortex and the cancellous interior.

Cancellous bone—The cancellous interior consists of secondary remodeled trabecular bone. The trabeculae extend far into the ornamental saddles (Fig. 7A), thus paralleling the external relief of the osteoderm.

Basal cortex—The basal cortex in both taxa consists of parallel-fibered bone (Fig. 7B) vascularized by few scattered simple primary vascular canals. Sharpey's fibers extensively insert into the cortical bone in oblique angles (range between 10° and 40°).

Paratypothorax (PEFO 5030, larger element; PEFO 34187, smaller element; TTU-P11594, fragment originally identified as *Calyptosuchus wellesi*)

External cortex—The cortex is composed of lamellar-zonal bone tissue, with resorption lines frequently reshaping the external saddle and valley ornamentation (Fig. 7C). Sharpey's fibers are concentrated in the saddle regions. The transition to the internal core area could be coarse cancellous or composed of Haversian bone, the latter being more strongly developed in PEFO 34187 than in PEFO 5030 and TTU-P11594. The general primary vascularization locally varies between reticular simple vascular canals and primary osteons, the latter can be closely spaced (Fig. 7D). In PEFO 5030, patches with up to five, hardly traceable growth marks were visible, whereas in PEFO 34187, a high number of tightly spaced growth marks (17–20 LAGs) were locally observed (Fig. 7E).

Cancellous bone—The core area is composed of secondary trabecular bone, but interstitial primary parallel-fibered bone tissue is also present (Fig. 7C–F).

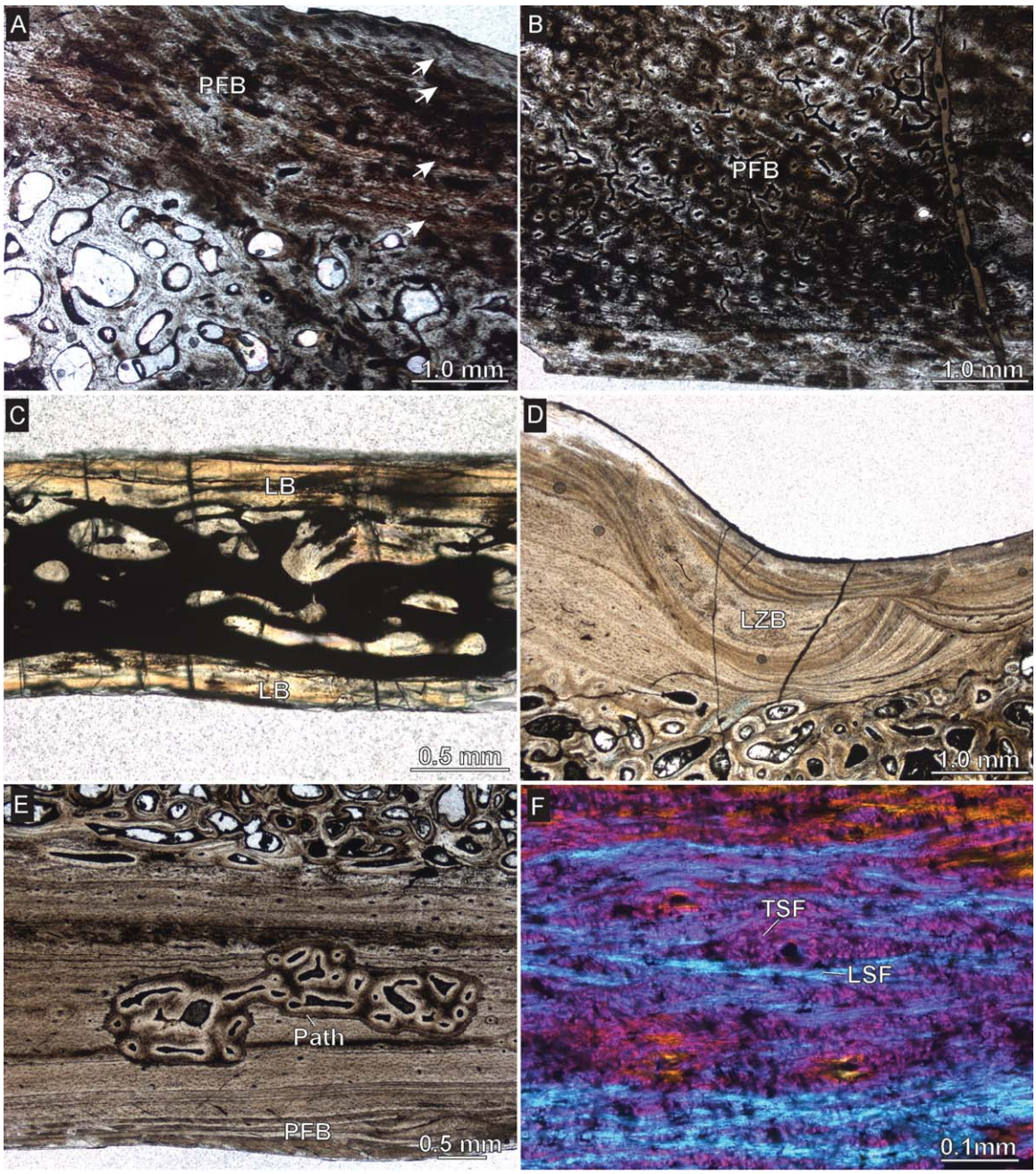

Fig. 6. Aetosaur osteoderm histology, part I. **A**,**B**: *Adamanasuchus eisenhardtae* (TTU-P10593). **C**: *Aetosaurus ferratus* (SMNS 12670). **D–F**: *Calyptosuchus wellesi* (PEFO 34191). Images in A–E are shown in normal polarized transmitted light, F in cross-polarized light using a lambda compensator. A: External cortex and interior trabecular bone tissue. Note growth marks (arrows) in compact bone. B: Basal cortex and interior non-trabecular bone tissue vascularized by reticular canal system. C: Complete view of sectioned thin osteoderm. Both cortices and the interior trabeculae consist of lamellar bone. D: External cortex and adjacent interior cancellous bone. Note resorption and redeposition of cortical bone tissue. E: Basal cortex and interior cancellous bone. Highly localized, presumably pathological pockets of secondary bone tissue are scattered within the cortex. No apparent connection to either the external bone surface or the interior was found. F: Close-up of the intercalated longitudinal and transverse fiber bundles constituting largely the more interiorly situated parts of the basal cortex. Abbreviations: LB, lamellar bone; LSF, longitudinally sectioned structural fibers; LZB, lamellar-zonal bone; PATH, pathological tissue; PFB, parallel-fibered bone; TSF, transversely sectioned structural fibers.

Basal cortex—The basal cortex consists of parallel-fibered bone, vascularized with primary vascular canals which can be rather evenly distributed lending the tissue a homogeneous appearance; no conspicuous coarse bundles of Sharpey's fibers are present. There is a clear, narrow transition between the internal core and the basal cortex, with few scattered secondary osteons invading the basal cortex tissue. Growth marks were not well enough

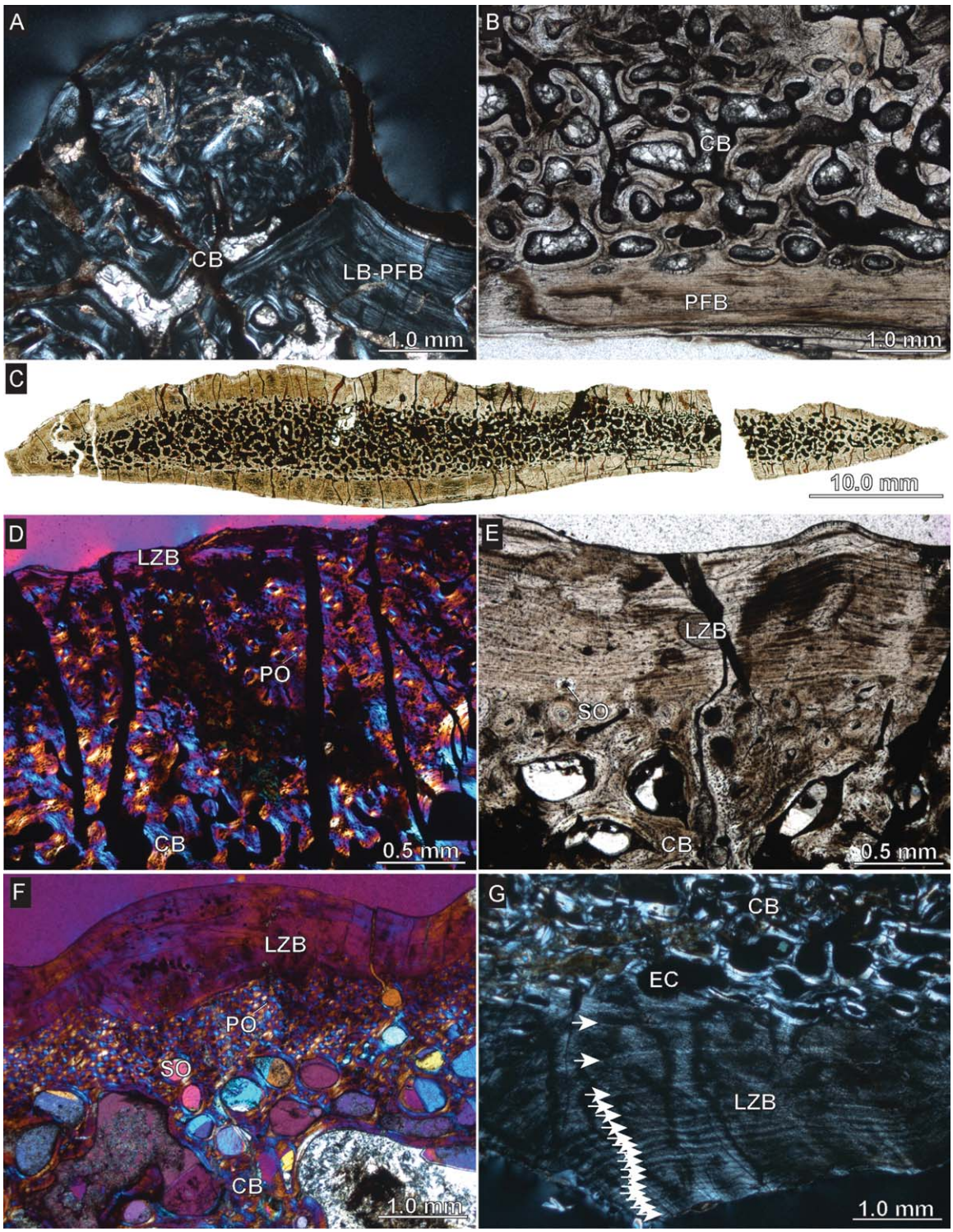

Fig. 7. Aetosaur osteoderm histology, part II. **A**,**B**: *Desmatosuchus smalli* (TTU-P09204-z). **C–F**: *Paratypothorax* (PEFO 5030, PEFO 34187, TTU-P11594). **G**: *Paratypothorax andressorum* (SMNS 91551). Images in A and G are shown in cross-polarized light, B, C, and E in normal polarized transmitted light, and D and F in cross-polarized light using a lambda compensator. A: Close-up of external cortex and ornamental ridge. B: Close-up of basal cortex and interior cancellous bone. C: Complete thin-section of PEFO 5030. D: Close-up of external cortex and interior cancellous bone. Note that outermost layers of lamellar-zonal bone have been largely eroded here leading to a scalloped surface relief. E: Close-up of external cortex and interior cancellous bone. F: Close-up of external cortex and interior cancellous bone. G: Close-up of basal cortex and interior cancellous bone. 17 Growth cycles are recognized (indicated by arrows), with the last 15 lines of arrested growth forming an outer circumferential layer or external fundamental system (e.g., Horner et al., 2000; Ponton et al., 2004). Abbreviations: CB, cancellous bone; EC, erosion cavity; LZB, lamellar-zonal bone; LB-PFB, lamellar bone grading into parallel-fibered bone; PFB, parallel-fibered bone; PO, primary osteon; SO, secondary osteon.

preserved to be counted in PEFO 5030 and TTU- P11594, but a minimum of 10 LAGs were counted in PEFO 34187.

Paratypothorax andressorum *(SMNS 91551, small thick fragment).* In this fragment from the anterior part of the osteoderm (the un-sculptured anterior bar), the histological details of the external and basal cortices appear to be very similar.

External cortex—The external cortex is composed of lamellar-zonal bone with coarse Sharpey's fibers inserting mostly perpendicularly into the bone surface. There is a narrow distinct border to the internal core area. The tissue is weakly vascularized with few scattered primary vascular canals, although a few scattered secondary osteons are also present.

Cancellous bone—The core is highly remodeled into thin and oblong trabeculae consisting of secondary lamellar bone.

Basal cortex—Lamellar-zonal bone with very few simple primary vascular canals is present, whereas conspicuous coarse bundles of Sharpey's fibers insert in moderate angles between 35° and 50° into the cortex. In areas where the compact bone is thickened, the best growth record is visible, showing growth zones and lines of arrested growth (a minimum of 17 growth cycles; Fig. 7G).

Stagonolepis olenkae *(ZPAL_Ab III-2379, one thinner and one thicker element).* Besides being from the type horizon and locality of *S. olenkae*, the species assignment appears valid because sampled specimens are spiked and not strongly curved in section, fitting well the species diagnosis given by Sulej (2010).

External cortex—The cortex is composed of lamellar bone (Fig. 8A,B). Locally coarse Sharpey's fibers are present extending over the lamellar bone tissue. The cortex is vascularized by scattered simple vascular canals and few scattered secondary osteons. Higher vascularization is restricted to areas of strong bone remodeling. The saddle and valley morphology of the surface ornamentation is also present in section as lines of resorption within the primary bone indicate successive cycles of bone erosion and deposition. Locally the ornamentation is deeply incised and at least six growth cycles (zones and annuli) could be counted in both specimens. One of the samples possesses an unusual deep excavation in the external cortex. This excavation is opened near the anterior margin of the osteoderm and extends within the external cortex in an antero-posterior orientation.

Cancellous bone—The core area is mostly composed of elongated slender secondary trabeculae, showing centripetally deposited lamellar bone (Fig. 8A).

Basal cortex—The basal cortex consists of lamellar-zonal bone, vascularized by a few scattered simple primary canals. Massive incorporation of coarse bundles of Sharpey's fibers is common. The Sharpey's fibers show a central point of inflection (fibers inverse direction), which is present in both sampled specimens (Fig. 8C). Similar to the external cortex, six growth cycles were counted, which were best visible at the lateral margin of the thinner element.

Stagonolepididae undescribed sp. (TTU-P18443-b, smaller fragment) and* Tecovasuchus chatterjeei *(TTU-P19902, large fragment). Following Martz and Small (2006), TTU-P19902 is identified as a *Tecovasuchus chatterjeei* paramedian osteoderm based on the presence of a raised anterior bar (also present in other species), an ornamentation combining deep circular pits and shallower radiating grooves (also in *Stagonolepis* and *Neoaetosauroides*) and posterior edge strongly thickened and beveled.

The paramedian osteoderm fragments are very similar in structure to that described already for the *Paratypothorax* specimens. They also show an external cortex which consists of lamellar-zonal bone (Fig. 8D,E) and a basal cortex of parallel-fibered bone, which is vascularized by a reticular network of primary vascular canals (Fig. 8F). The cortices frame an interior core area of secondary remodeled trabecular bone. Up to five growth cycles (growth zones separated by LAGs) are countable in the external cortex of TTU-P19902, whereas in the basal cortex only two growth cycles (growth zones and annuli) are visible due to strong remodeling of the primary bone tissue. Sharpey's fibers are not conspicuous in this specimen and only found in few patches in the external and basal cortices. In TTU-P18443-b, eight or nine growth cycles (mostly indicated by LAGs) are countable in both the external and basal cortices. Fine Sharpey's fibers are also widely discernible throughout the external but more patchily in the basal cortices in this specimen.

Typothorax *(PEFO 5039 large fragment, originally referred to as* Typothorax *cf.* T. coccinarum*; PEFO 36853, large osteoderm; SMNS 91550, smaller fragment).* Osteoderms of three different sizes were sampled. The smallest specimen is SMNS 91550, the larger ones PEFO 5039 and 36853, with the latter of the two being more completely preserved. All three specimens show the flat external surfaces with non-radiating ornamentation consisting of sub-circular pits surrounded by ridges, and prominent keels on the basal sides typical for *Typothorax* paramedian osteoderms. Based on their fragmentary nature (i.e., length to width ratios not known), however, none could be unambiguously assigned to a species. The finer and denser external pitting patterns in PEFO 5039 and the specimen from SMNS would generally favor an assignment to *T. coccinarum* instead of *T. antiquum* (see Parker and Martz, 2011). All specimens share the most complex histological structure among all sampled aetosaur osteoderms, including published data on *Aetosauroides scagliai* (Cerda and Desojo, 2011) and the desmatosuchine *Sierritasuchus macalpini* (Parker et al. 2008).

Smaller Osteoderm (SMNS 91550)

In the anterior bar region, the bone is compact and a diploe structure is not yet developed. Here the bone tissue consists of parallel-fibered bone, vascularized with an extensive reticular system of primary vascular canals (Fig. 9A). The canals are larger in the central area of the bar and decrease in diameter towards the outer bone surface. Towards the anterior tip of the bar the layers of parallel-fibered bone extend sub-parallel to the external, lateral, and basal bone surfaces. A diploe structure (described in detail below) is developed at the thickened central and more posteriorly situated regions of the

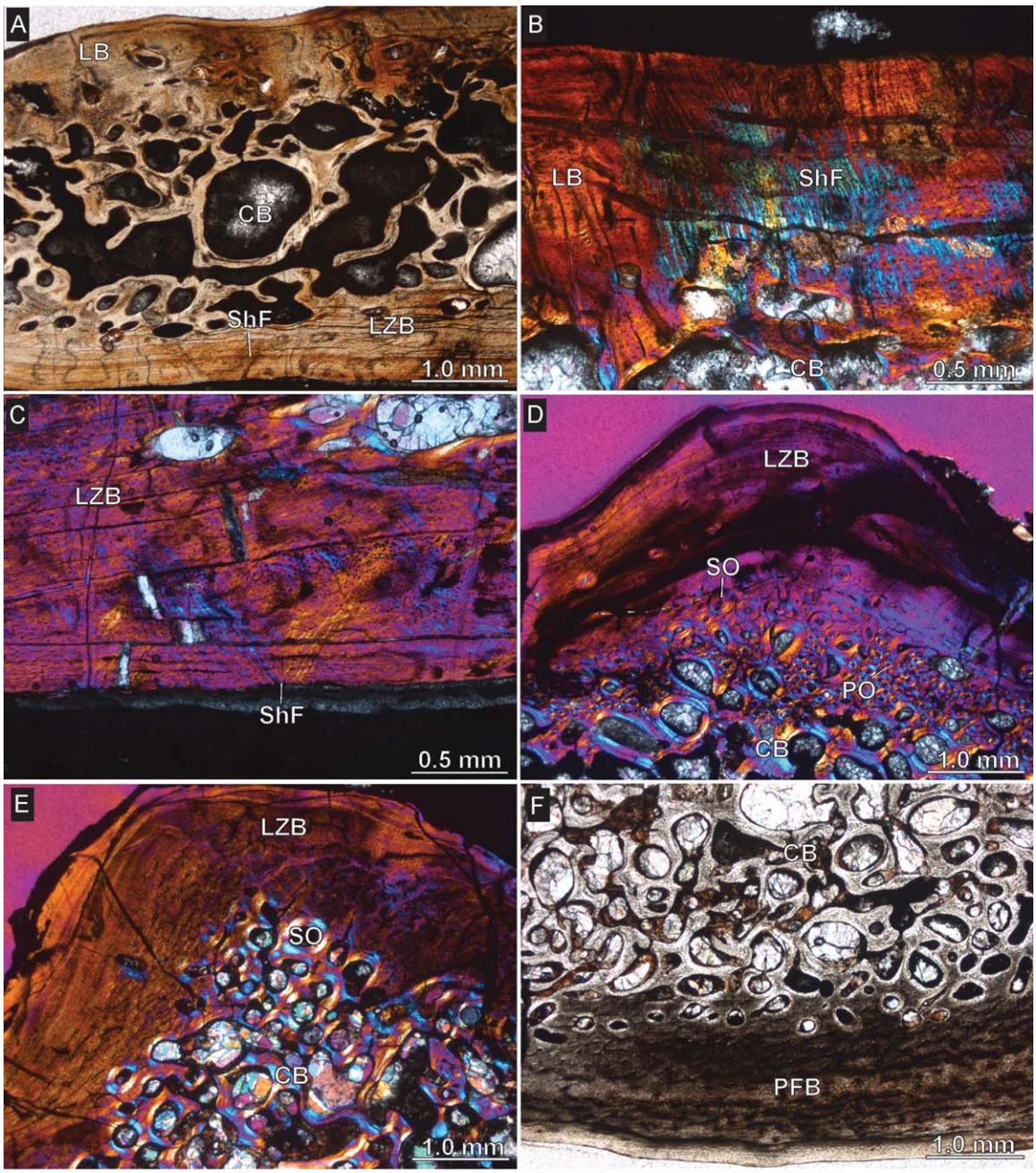

Fig. 8. Aetosaur osteoderm histology, part III. **A–C**: *Stagonolepis olenkae* (ZPAL Ab III/2379). **D**: Stagonolepididae unnamed sp. (TTU-P18443-b). **E**,**F**: *Tecovasuchus chatterjeei* (TTU-P19902). Images in A and F are shown in normal polarized transmitted light, B–E in cross-polarized light using a lambda compensator. A: Diploe structure of the osteoderm. B: Close-up of the external cortex showing strong incorporation of coarse Sharpey's fibers. C: Close-up of the basal cortex with the "inflection" point of differently arranged oblique Sharpey's fiber sets (bluish and yellowish colors). D,E: Close-up of the external cortex and interior cancellous bone. F: Close-up of the basal cortex and interior cancellous bone. Abbreviations: CB, cancellous bone; LB, lamellar bone; LZB, lamellar-zonal bone; PFB, parallel-fibered bone; PO, primary osteon; ShF, Sharpey's fibers; SO, secondary osteon.

osteoderm (Fig. 9B), whereas the posterior margin of the osteoderm is yet more compact again (Fig. 9C).

External cortex—The external cortex shows an external ornamentation of ridges and valleys in various stages of remodeling. Lines of resorption mark separate areas of secondary bone deposition, which consist locally of parallel-fibered or fibro-lamellar bone, the latter showing also plumper and round cell lacuna shapes (Fig. 9D). Patches with irregular growth marks (three LAGs and annuli could be identified) are present only in the external-most parts of the cortex, but they cannot be followed through the section, thus preventing reliable counts.

Cancellous bone—In the central thickened core region, trabecular bone is developed consisting of few thick

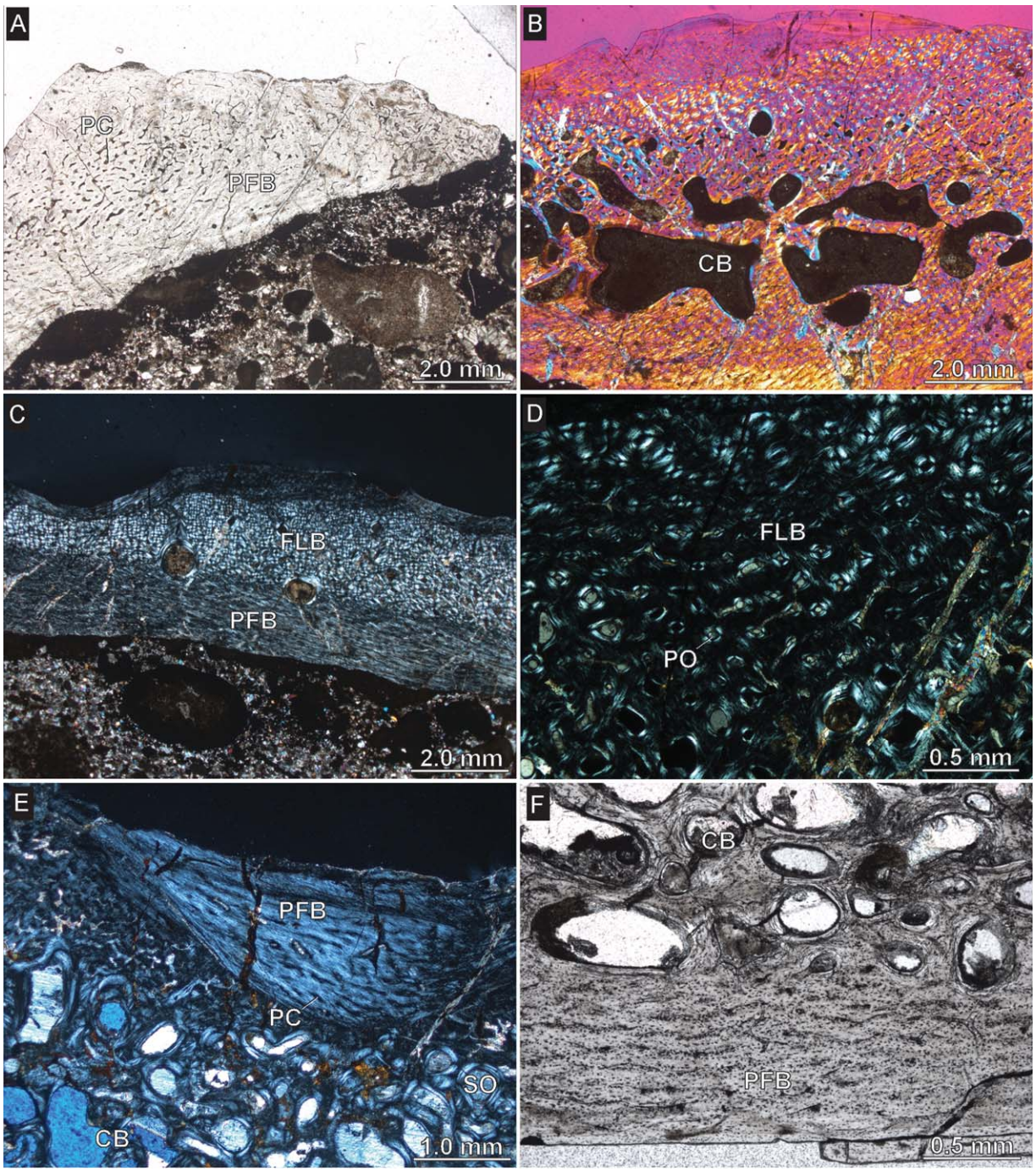

Fig. 9. Aetosaur osteoderm histology, part IV. **A–D**: *Typothorax* (SMNS 91550). **E–F**: *Typothorax* (PEFO 36853). Images in A and F are shown in normal polarized transmitted light, B in cross-polarized light using a lambda compensator, and C–E in cross-polarized light. A: Anterior bar region. B: Thickened central region. C: Close-up of most posteriorly situated region. D: Close-up of external cortex being composed of fibro-lamellar bone. E: Close-up of external cortex and interior cancellous bone. F: Close- up of basal cortex and interior cancellous bone. Abbreviations: CB, cancellous bone; FLB, Fibro-lamellar bone; PC, primary vascular canal; PFB, parallel-fibered bone; PO, primary osteon.

primary trabeculae and irregularly shaped intertrabecular erosion cavities. Sporadic deposition of secondary lamellar bone lines the vascular spaces. Primary bone consists of parallel-fibered and fibro-lamellar bone, the latter being prominently deposited in areas adjacent to the external cortex. In the more posteriorly situated parts of the osteoderm, the trabeculae and large erosion cavities are substituted by a finer scaffolding of primary trabecular bone highly vascularized by densely packed primary osteons and smaller erosion cavities lined with

secondary lamellar bone (resembling large secondary osteons). Towards the posterior margin of the osteoderm, the smaller erosion cavities disappear and are themselves substituted by a few scattered secondary osteons. The interior of the osteoderm can be completely composed of fibro-lamellar bone vascularized by tightly packed primary osteons (Fig. 9C,D). The posterior-most tip of the osteoderm shares the same histological structures as the anterior bar in that a diploe structure is missing and that the bone tissue is vascularized by a reticular network of primary canals. However, the layers do not extend sub-parallel to the osteoderm surfaces, so that the parallel-fibered bone of the basal cortex can be clearly separated from the internal core and external compact bone, the latter two being composed of parallel-fibered and fibro-lamellar bone.

Basal cortex—The cortex is composed of parallel-fibered bone well vascularized with simple primary vascular canals, which extend predominantly sub-parallel to the basal bone surface. In the central area of the osteoderm, the canals are more randomly arranged in the cortex, with a single layer of avascular parallel-fibered bone intercalating with the rest of the parallel-fibered bone. No growth marks could be counted in the basal cortex.

Larger Osteoderms (PEFO 5039, 36853)

The PEFO specimens resemble, to a large part, the histological description of the smaller SMNS 91550 specimen in that, for example, (a) the basal cortex is mainly composed of parallel-fibered bone vascularized by a network of primary canals and that (b) the valleys and saddles of the external cortex are composed of numerous remodeled parts of parallel-fibered and fibro-lamellar bone (Fig. 9E). The main difference between the specimens, however, is the well-developed diploe structure being present only in the PEFO specimens. Here the sub-equally thick external and basal compact layers, which surround the internal core, extend almost from the tip of the anterior bar to the posterior margin of the osteoderm. At the anterior-most tip and the posterior margin, however, the cancellous bone almost reaches the basal bone surface, thus the thickness ratio between the external and basal compacta shifts towards 3:1 or even 4:1. Large areas of the osteoderm center and the primary external cortex have been extensively remodeled. They now consist of secondary trabecular bone constituting centripetally deposited lamellar bone (Fig. 9E), whereas the basal cortex consists of parallel-fibered bone (Fig. 9F). Although areas preserving growth cycles are more widespread in the PEFO specimens, growth marks remain untraceable throughout the complete sections. Locally, 10–12 LAGs were counted in the cortex of PEFO 5039.

Outgroup Comparison

Revueltosaurus callenderi *(PEFO 35283, thin element)*. Besides stratigraphic reasons, the specimen is identifiable as a *R. callenderi* paramedian osteoderm, based on having the sub-rectangular outline with an anterior bar and "subcircular pitting arranged in a random to weakly radial pattern" as noted by Parker et al. (2005; compare also to referred osteoderm shown in fig. 3g).

The element has a rather compact structure, with both external and basal cortices well developed. Although some large resorption cavities can be observed at the internal core of the osteoderm, a distinct cancellous bone is not developed in this area. Growth marks, that is, 11 LAGs are present (Fig. 10A), although they are more pronounced in polished section and more difficult to trace within thin-sections, mostly because of internal remodeling processes.

External cortex—The cortex shows parallel-fibered bone. Sharpey's fibers insert perpendicularly to the external bone surface into the primary bone tissue. The external ornamentation pattern consists of valleys and saddles, which involved the resorption of primary parallel-fibered bone and re-deposition of lamellar bone (Fig. 10B,C) in drifting ornamentation pits (*sensu* Buffrénil, 1982). In thin-section and one polished longitudinal section, 11 LAGs were counted.

Internal core—The core area consists of primary parallel-fibered tissue densely remodeled by secondary osteons and secondary vascular canals resembling secondary osteons.

Basal cortex—The cortex consists of parallel-fibered bone. Growth marks hinting at a zonation of the tissue are not conspicuous. Sharpey's fibers are few, inserting in low to moderate angles (20° to 40°) into the bone proper. Most layers of the parallel-fibered bone are avascular but very few scattered primary vascular canals are present throughout the whole of the cortex.

Jaxtasuchus salomoni *(SMNS 81902, SMNS 91549): (thicker osteoderm, PHZ 12; thinner osteoderm, PHZ 14)*. In addition to be from the type locality and listed among the referred material in Schoch and Sues (2013), the identification of the specimens as *J. salomoni* paramedian osteoderms appears valid based on their overall rectangular outline, an ornamentation pattern "comprising prominent ridges and deep pits that are more strongly developed but fewer in number than on comparable osteoderms of *Doswellia*", and having a "distinct dorsal eminence of variable shape", the latter characteristic being shared with *Doswellia* (Schoch and Sues, 2013: p. 2).

The cortices are of similar thickness and the diploe structure is restricted to thicker, central cores of the osteoderms. The lateral parts show a more compact structure with converging cortices framing only thin intercalated central layers which, in longitudinal section, are well vascularized with reticular primary canals and primary osteons (Fig. 10D).

External cortex—The cortex, its bone tissue consisting of parallel-fibered bone, is strongly sculptured into valleys and saddles. Resorption lines hint at the remodeling of previously deposited external compact layers (Fig. 10E). The relief of the surface ornamentation increases through differential growth throughout the cortex. The cortex is extensively vascularized by a reticular network of primary vascular canals and scattered larger foramina insert into more central areas of the osteoderms. Sharpey's fibers usually insert perpendicular to the bone surface into the tissue. They occur both at saddles and valleys. The external-most layers of the cortex are avascular and show a good growth record. In SMNS 81902, six to eight growth cycles (zones and LAGs/annuli) were

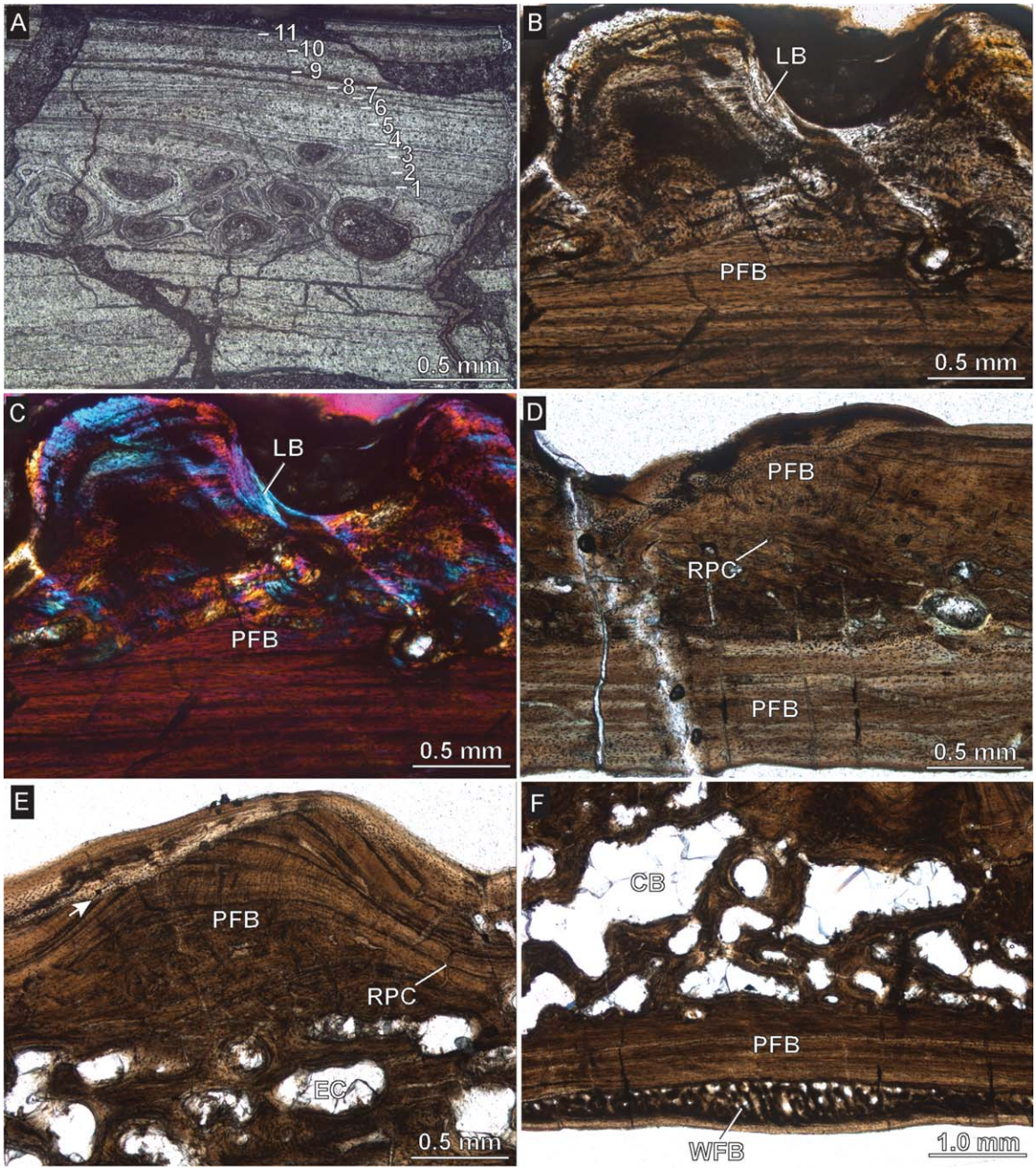

Fig. 10. Osteoderm histology of outgroup taxa. **A–C**: *Revueltosaurus callenderi* (PEFO 35283). **D–F**: *Jaxtasuchus salomoni* (SMNS 81902, SMNS 91549). Image in A shows polished section in reflected light. Images in B and D–F are shown in normal polarized transmitted light, C in cross-polarized light using a lambda compensator. A: Eleven growth marks (lines of arrested growth) are identified in the external cortex. B,C: Close-up of the external cortex. Note erosion of primary bone and deposition of lamellar bone at the margin of ornamental pit. D: Part of longitudinal section of specimen. E: Close-up of external cortex showing resorption of earlier growth stages and subsequent bone deposition (arrow). Note relief of surface ornamentation increasing through differential growth. F: Close-up of interior cancellous bone and basal cortex with localized pad of highly vascularized woven bone tissue. Abbreviations: CB, cancellous bone; EC, erosion cavity; LB, lamellar bone; PFB, parallel-fibered bone; RPC, reticular primary vascular canals; WFB, woven-fibered bone.

counted, whereas in SMNS 91549 no more than three were countable.

Cancellous bone—The internal core shows trabecular bone with short thick primary trabeculae and small inter-trabecular spaces only where the osteoderm is thickest (Fig. 10E,F). The trabeculae consist of primary parallel-fibered bone tissue lined with secondary lamellar bone. Thickened areas of internal bone tissue with extensive reticular vascularization are present deep to each external saddle. The parallel-fibered bone of the core area generally has a different, slightly more isotropic extinction pattern (well visible in polarized light

with lambda compensator) than the surrounding cortical parallel-fibered bone.

Basal cortex—The basal cortex consists of parallel-fibered bone. In SMNS 91549, the cortex is vascularized by scattered simple and reticular primary vascular canals. In SMNS 81902, vascularization was less pronounced with only few scattered simple primary vascular canals. Sharpey's fibers insert in low to moderate angles (range between 20° and 50°) into the cortical tissue in both specimens. They are extending predominantly towards the thicker central core area of the osteoderm, as is visible in longitudinal section. Four growth cycles could be found in SMNS 81902.

Below the keel region of the specimen, the basal-most layer of the cortex shows a localized patch of highly vascularized, woven fibered tissue surrounded by the parallel-fibered layers (Fig. 10F). Vascular spaces are primary, reticular, and not widened by additional resorptive processes, whereas towards the tapering margins of the patch, vascularization is mainly by reticular network of smaller primary canals. Osteocyte lacunae are enlarged and circular here compared to the more oblong ones in the surrounding bone layers. Sharpey's fibers are also embedded within the irregular tissue patch, thus appearing to be continuous with those in the surrounding parallel-fibered bone. This layer of woven fibered bone resembles the pathological, reactive bone tissue observed in other archosaurs (Reid, 1996; Chinsamy and Tumarkin-Deratzian, 2009).

DISCUSSION

The phytosaur and aetosaur osteoderms sampled herein are usually less compact in comparison to "rauisuchian" osteoderms (Scheyer and Desojo, 2011; Cerda et al., 2013), and all specimens show a diploe structure in which a central cancellous core is surrounded by compact bone layers.

In phytosaurs, growth stages of the osteoderms are usually clearly visible (except in the sampled Phytosauria SMNS 91013 and *Pseudopalatus* osteoderms), with growth counts often being easier to perform with higher levels of reproducibility. These are thus deemed to be more reliable than growth counts in the aetosaur osteoderms. The external and basal cortical tissues are very similar in structure, in most cases showing a succession of strongly vascularized growth zones intercalated with less vascularized layers, both composed of parallel-fibered bone (only in *Paleorhinus* the less vascularized parts consisted of zones of lamellar bone). The amount and structure of Sharpey's fibers, however, differs between external and basal cortices. Particularly in the basal cortex, insertion and extension of coarser bundles of Sharpey's fibers was reminiscent of those seen in crocodylian osteoderms, so that a functional incorporation of paramedian osteoderms into the axial bracing system (*sensu* Frey, 1988) is also plausible in phytosaurs. The differences encountered by Scheyer and Sander (2004) between the Phytosauria osteoderm (IPB R479) and crocodylian osteoderms thus appear to be related to the fact that the former is an appendicular osteoderm (also differing from the other phytosaurs sampled herein) and not a paramedian osteoderm from a paravertebral shield (*sensu* Frey, 1988; Salisbury and Frey, 2001). Otherwise, we do confirm the observation of Scheyer and Desojo (2011) and Cerda et al. (2013) that the pitting ornamentation pattern observable in crocodylian osteoderms, and which was recognized now also in *Revueltosaurus*, is not found in any aetosaur or phytosaur osteoderm so far.

Among the aetosaurs, even the thinnest and smallest specimen sampled, that is, SMNS 12670, presumably from a juvenile *Aetosaurus ferratus*, shows a diploe structure. Depending on the individual thickness of the osteoderms, the cancellous part can be quite extensive. External and basal compact bone layers are generally of similar thickness. The histological variation (including the extent of interior cancellous core area) observed in the three different sized *Typothorax* osteoderms herein is interpreted to represent different ontogenetic stages of the individuals sampled. This stands in contrast to the basal aetosaur osteoderms (incl. *Aetosauroides scagliai*) from South America sampled by Cerda and Desojo (2011), which generally lacked a larger area of internal cancellous bone. In a recent contribution, Taborda et al. (2013) showed that the *Aetosauroides scagliai* osteoderms (paramedian and laterals) maintained a rather compact structure through its ontogeny. Hence, our data reinforces the previous hypothesis proposed by Cerda and Desojo (2011), who suggested that the compact microanatomy of the *A. scagliai* was a typical feature of this taxon.

Given the presence of a well-developed core of cancellous bone tissue in most aetosaurian osteoderms, the estimation of the absolute age of the individuals from growth mark counting alone appears to not be possible. The age values obtained from this method are necessarily a minimum age because of secondary remodeling of the internal core. Cerda and Desojo (2011) proposed that Aetosaurinae aetosaurian osteoderms appear to be well suited to infer absolute age in these archosaurs. Our data indicate that it is true only in those taxa where the secondary remodeling of the internal core is minimal or absent (i.e., in *A. scagliai*).

In the case of the *Paratypothorax* specimens from North America and Europe, cortical and overall thickness of the specimens indicate similar osteoderm sizes—this assumption is corroborated by similar growth mark counts of 17–20 LAGs.

The paramedian osteoderm of *Adamanasuchus eisenhardtae* shared a general histological structure with the other aetosaur samples, but it also differed somewhat in its interior cancellous composition. However, given the limited amount and fragmentary nature of the material, it is not clear if these interior structures are apomorphic for the species or if they are variable among individuals. More and less fragmentary material will shed light on this problem.

Some of the aetosaur osteoderms seem to express histological features that are potentially apomorphic for a species/genus, such as the overall complex built of the *Typothorax* osteoderms and the internal structure of the basal cortex (i.e., loose, intercalated longitudinally and transversely arranged fibers) in *Calyptosuchus wellesi* (PEFO 34191). Specimen TTU-P11594 lacked this histological structure but shows details consistent with the *Paratypothorax* specimens PEFO 5030 and 34187. Therefore, based on outer morphology (e.g., radiating ornamental ridges as in lateral parts of *Paratypothorax* paramedian osteoderms, lack of keel on basal side of osteoderm) and histology, we confidently identify this

specimen as belonging to *Paratypothorax* instead of *Calyptosuchus*. In addition, *Tecovasuchus* and the yet to be described stagonolepidid species were found to be very similar to *Paratypothorax* in terms of its osteoderm histology, although outer morphological characters clearly differentiate all three taxa.

Stagonolepis olenkae from Poland showed very coarse Sharpey's fibers in its external cortex and two sets of oblique Sharpey's fibers partly overlapping each other in the basal cortex, with the latter also commonly found in modern crocodylian osteoderms. In the extant crocodilians, the Sharpey's fiber arrangement pertains to the attachment of the myosepta of epaxial musculature and marginally the interosteodermal and cingulate ligaments into the basal osteoderm cortex (e.g., Salisbury and Frey, 2001; Schwarz-Wings et al., 2009). The Sharpey's fiber arrangement in *S. olenkae* might thus indicate a strong integration of the paramedian osteoderms into the vertebral bracing system of the animal as in modern crocodylians.

Revueltosaurus is characterized by an overall compact osteoderm structure and the presence of parallel-fibered bone tissue in all areas of the bone. Even though it is quite small in dimensions and definitely thinner than some of the other osteoderms sampled herein, it nevertheless showed a high amount of growth cycles, indicating that the animal was in its twelfth year of life (thirteenth year of life if, as in crocodylians, osteoderm mineralization sets in well after hatching; Vickaryous and Hall, 2008). Its position as sister taxon to aetosaurs indicates that faster growth rates, as indicated by the presence of woven or fibro-lamellar bone in several aetosaur taxa (e.g., in the basal *Aetosauroides* and the more highly nested *Calyptosuchus* and *Typothorax*), were not necessarily inherited along the lineage leading to Aetosauria. Instead they might have evolved independently and repeatedly within Aetosauria. In comparison, fibrolamellar bone was encountered only in a single phytosaur osteoderm (TTU-P19255) sampled herein (although the sample size of phytosaur osteoderms was much lower).

Similar to the *Revueltosaurus* osteoderm, the doswelliid *Jaxtasuchus salomoni* samples are also characterized by a general parallel-fibered bone matrix and a good growth record. Both features have also been reported in a recently preliminary study (Cerda et al., 2011) of the osteoderms of *Chanaresuchus ischigualastensis*, a proterochampsid from the early late Triassic from Argentina (Trotteyn et al., 2012). The localized patch of faster growing bone in the basal cortex of specimen SMNS 81902 indicates, however, the potential for faster bone deposition under certain conditions (whether as primary deposits or as a reaction to trauma, bone lesion or infection cannot be elucidated).

The data obtained from our sample (Fig. 1) and from previous studies allow us to compare the osteoderm microstructure of aetosaurs, phytosaurs, *Jaxtasuchus*, and *Revueltosaurus* with other archosauriform taxa, particularly of the pseudosuchian lineage. Since the external microanatomy of pseudosuchian osteoderms is variable even within a single species, we only compare their fine internal histology. The basal cortex of pseudosuchians is commonly composed of parallel-fibered bone tissue (Hill and Lucas, 2006; Scheyer and Sander, 2004; Parker et al., 2008; Vickaryous and Hall, 2008; Vickaryous and Sire, 2009; Klein et al., 2009; Hill, 2010; Cerda and Desojo, 2011; Scheyer and Desojo, 2011; Filippi et al., 2013). In "rauisuchians" and crocodylomorphs (subclade of Paracrocodylomorpha in Fig.1), the internal core (when not remodeled) is composed of parallel-fibered, woven-fibered, and/or fibro-lamellar bone tissues. Woven-fibered and fibro-lamellar bone was also described in the osteoderm internal core of aetosaurs as, for example, in *Typothorax*, and in the non-archosaurian archosauriform *Jaxtasuchus*. Mineralized structural fiber bundles have been reported in the internal core of some taxa of "rauisuchians", crocodylomorphs, and phytosaurs (Hill and Lucas, 2006; Scheyer and Sander, 2004; Vickaryous and Hall, 2008; Vickaryous and Sire, 2009; Klein et al., 2009; Cerda and Desojo, 2011; Scheyer and Desojo, 2011), but so far never in Aetosauria, *Revueltosaurus*, and *Jaxtasuchus*. The presence of such fibers in the internal core areas has been interpreted as evidence of a metaplastic origin of the osteoderms in several archosauriform lineages (Scheyer and Sander, 2004; Vickaryous and Hall, 2008; Cerda and Powell, 2010; Scheyer and Desojo, 2011). As pointed out by Cerda and Desojo (2011), the absence of structural fibers in the internal core of aetosaur osteoderms suggests that these bones were not initially formed by metaplasia but by intramembraneous ossification. The structural fibers recorded in the basal cortex of *Calyptosuchus wellesi* were possibly incorporated into the osteoderm late during ontogeny by metaplasia of the dermis. The current evidence thus suggests that the osteoderms were originated by metaplasia mainly in phytosaurs, some "rauisuchians" and crocodylomorphs.

The microstructure of the external cortex is variable in pseudosuchians. It is mostly composed by lamellar and parallel fibered bone, but some degree of variation occurs, even in a single clade or lineage (e.g., crocodylomorphs). For example, whereas the external cortex of the "rauisuchian" osteoderms does not reveal any processes of resorption and new deposition of periosteal bone, this process is actually well recorded in aetosaurs, several crocodylomorph taxa, as well as in *Jaxtasuchus* and *Revueltosaurus*. This process of resorption and redeposition of the bone tissue is evident in taxa where osteoderms possess a strong ornamentation (deep pits and grooves), but is absent in elements with a more delicate external ornamentation. Hence, this histological variation appears to be related to the degree of ornamentation of the superficial surface. The patchy distribution of this character within Archosauriformes suggests independent losses (at least in phytosaurs and "rauisuchian" pseudosuchians, Fig. 1) during the evolution of this lineage.

CONCLUSIONS

This is the first comparative study on the osteohistology of phytosaur and aetosaur osteoderms. In contrast to the assumption of Scheyer and Desojo (2011), fibrolamellar and woven bone tissues which indicate higher bone growth rates are known now from a variety of pseudosuchian and archosauriform osteoderms, including Phytosauria, Aetosauria, "Rauisuchia", and archosauriforms situated more basally on the tree. These tissues are not obligatorily found in all species of each group but are independently developed by some taxa.

This is consistent with studies on the long bone histology of these animals, which indicate that the physiological prerequisites for the high growth rates found in dinosaurs and birds (e.g., Ricqlès et al., 2003) evolved already non-simultaneously earlier within the archosauromorph lineage (Werning et al., 2011). As evidenced by the *Typothorax* specimens, osteoderm thickness and the cancellous to compact bone ratio appear to be subject to ontogenetic change. So far, histological evidence (of osteoderm core areas) suggests a metaplastic origin for a few phytosaur (and "rauisuchian") osteoderms, but not for aetosaurs, *Revueltosaurus*, and *Jaxtasuchus*. Minimum growth mark counts in osteoderms sampled herein indicate that some aetosaurs and phytosaurs lived at least for two decades. Bone microstructures are more uniform in phytosaur osteoderms and show a higher level of disparity among aetosaur osteoderms. Moreover, if we compare our aetosaurian sample with previous studies (e.g., Cerda and Desojo, 2011), the histological variation within Aetosauria increased with the amount of taxa studied. Thus, inter- and intraspecific studies among aetosaur taxa are needed to better understand the breadth of histostructures present in this fossil lineage.

ACKNOWLEDGEMENTS

We especially thank Rainer Schoch (SMNS, Stuttgart, Germany), William Parker (PEFO, Petrified Forest, Arizona), Thomas Sulej (PAN, Warszawa, Poland), Bill Mueller, Matt Renick and Sankar Chatterjee (TTU, Lubbock, Texas), and Martin Sander (Steinmann Inst., Univ. Bonn, Germany) for access to specimens under their care. Michelle Stocker (Univ. of Texas, Austin), Rainer Schoch (Germany), and Bill Mueller (USA) are thanked for discussions. Thanks also to Julia Huber, Leonie Paulie, Fiona Straehl, and Vivien Jaquier (all Zurich, Switzerland) for preparing and photographing specimens and thin-sections. Two anonymous reviewers offered comments that greatly improved earlier versions of the manuscript. This work was funded by the Swiss National Science Foundation (No. 31003A 146440 to TMS), the Agencia Nacional de Promoción Científica y Técnica (PICT 2012 N° 925 to JBD and IAC), and Alexander von Humboldt Foundation (to JBD).

LITERATURE CITED

Ballew KL. 1989. A phylogenetic analysis of Phytosauria from the Late Triassic of the Western United States. In: Hunt AP, Lucas SG, editors. Dawn of the Age of Dinosaurs in the American Southwest. Albuquerque, New Mexico: New Mexico Museum of Natural History. p 309–339.

Brusatte SL, Benton MJ, Desojo JB, Langer MC. 2010. The higher-level phylogeny of Archosauria (Tetrapoda: Diapsida). J Syst Palaeontol 8:3–47.

Buchwitz M, Witzmann F, Voigt S, Golubev V. 2012. Osteoderm microstructure indicates the presence of a crocodylian-like trunk bracing system in a group of armoured basal tetrapods. Acta Zool (Stockh) 93:260–280.

Buffetaut E. 1993. Phytosaurs in time and space. Paleontologia Lombarda N. S. 2:39–44.

Buffrénil V de . 1982. Morphogenesis of bone ornamentation in extant and extinct crocodilians. Zoomorphology 99:155–166.

Case, E. C. 1920. Preliminary description of a new suborder of phytosaurian reptiles with a description of a new species of *Phytosaurus*. J Geol 28:524–535.

Cerda IA, Powell JE. 2010. Dermal armor histology of *Saltasaurus loricatus*, an Upper Cretaceous sauropod dinosaur from Northwest Argentina. Acta Palaeontol Pol 55: 389–398.

Cerda IA, Desojo JB. 2011. Dermal armour histology of aetosaurs (Archosauria: Pseudosuchia), from the Upper Triassic of Argentina and Brazil. Lethaia 44:417–428.

Cerda IA, Desojo JB, Scheyer TM, Schultz CL. 2013. Osteoderm microstructure of "rauisuchian" archosaurs from South America. Geobios 46: 273–283 [doi: 10.1016/j.geobios.2013.01.004].

Cerda IA, Trotteyn MJ, Desojo JB. 2011. Microestructura ósea de los osteodermos de *Chanaresuchus* (Archosauriformes: Proterochampsidae) de la Formacion Ischigualasto (Triásico Superior) de Argentina. Ameghiniana 4:8R.

Chatterjee S. 1978. A primitive parasuchid (phytosaur) reptile from the Upper Triassic Maleri Formation of India. Palaeontology 21:83–127.

Chinsamy A., Raath MA. 1992. Preparation of fossil bone for histological examination. Palaeontol Afr 29:39–44.

Chinsamy-Turan A. 2005. The Microstructure of Dinosaur Bone. Baltimore: Johns Hopkins University Press.

Chinsamy A, Tumarkin-Deratzian A. 2009. Pathologic bone tissues in a turkey vulture and a nonavian dinosaur: implications for interpreting endosteal bone and radial fibrolamellar bone in fossil dinosaurs. Anat Rec 292:1478–1484.

Cope ED. 1875. Report on the geology of that part of northwestern New Mexico examined during the field-season of 1874. In: Annual Report upon the geographical explorations west of the 100th Meridian [Wheeler Survey], Appendix LL, Annual Report Chief of Engineers for 1875, 61–97 of separate issue, 981–1017 of full report.

Desojo JB, Ezcurra MD. 2011. A reappraisal of the taxonomic status of *Aetosauroides* (Archosauria, Aetosauria) specimens from the Late Triassic of South America and their proposed synonymy with *Stagonolepis*. J Vertebr Paleontol 31:596–609.

Desojo JB, Ezcurra MD, Kischlat EE. 2012. A new aetosaur genus (Archosauria: Pseudosuchia) from the early Late Triassic of southern Brazil. Zootaxa 3166:1–33.

Desojo JB, Heckert AB, Martz JW, Parker WG, Schoch RR, Small BJ, Sulej T. 2013. Aetosauria: a clade of armoured pseudosuchians from the Late Triassic continental beds. In: Nesbitt SJ, Desojo JB, Irmis RB, editors. Anatomy, Phylogeny and Palaeobiology of Early Archosaurs and their Kin. Geol Soc Lond Spec Publ 389:203–239 [doi:10.1144/SP379.17].

Farlow, JO, Hayashi S, Tattersall GJ. 2010. Internal vascularity of the dermal plates of *Stegosaurus* (Ornithischia, Thyreophora). Swiss J Geosci 103:173–185.

Filippi LS, Cerda IA, Garrido AC. 2013. Morfología e histología de osteodermos de un Peirosauridae de la Cuenca neuquina. Ameghiniana 50:3–13.

Fraas O. 1877. *Aetosaurus ferratus* Fr. Die gepanzerte Vogel-Echse aus dem Stubensandstein bei Stuttgart. Festschrift zur Feier des vierhundertjährigen Jubilaums der Universität Tübingen. Jahresh Ver Vaterl Naturkd Wuerttemb 33:1–21.

Frey E. 1988. Das Tragsystem der Krokodile—eine biomechanische und phylogenetische Analyse. Stuttg Beitr Naturkd (A Biol) 426:1–60.

Gregory JT. 1962. The genera of phytosaurs. Am J Sci 260:652–690.

Hayashi S, Carpenter K, Watabe M, McWhinney LA. 2012. Ontogenetic histology of Stegosaurus plates and spikes. Palaeontology 55:145–161.

Heckert AB, Lucas SG. 2000. Taxonomy, phylogeny, biostratigraphy, biochronology, paleobiogeography, and evolution of the Late Triassic Aetosauria (Archosauria:Crurotarsi). Zbl Geol Paläont Teil I (11-12):1539–1587.

Heckert AB, Lucas SG. 2002. South American occurrences of the Adamanian (Late Triassic: Latest Carnian) index taxon *Stagonolepis* (Archosauria: Aetosauria) and their biochronological significance. J Paleontol 76:852–863.

Hill RV. 2005. Integration of morphological data sets for phylogenetic analysis of Amniota: the importance of integumentary characters and increased taxonomic sampling. Syst Biol 54: 530–547.

Hill RV. 2010. Osteoderms of *Simosuchus clarki* (Crocodyliformes: Notosuchia) from the Late Cretaceous of Madagascar. J Vertebr Paleontol 30:Suppl:6 (SVP Memoir 10):154–176 [doi:110.1080/02724634.02722010.02518110].

Hill RV, Lucas SG. 2006. New data on the anatomy and relationships of the Paleocene crocodylian *Akanthosuchus langstoni*. Acta Palaeontologica Polonica 51:455–464.

Hillebrandt AV, Krystyn L. 2009. On the oldest Jurassic ammonites of Europe (Northern Calcareous Alps, Austria) and their global significance. N Jb Geol Palaeont Abh 253:163–195.

Horner JR, de Ricqlès A, Padian K. 2000. Long bone histology of the hadrosaurid dinosaur *Maiasaura peeblesorum*: growth dynamics and physiology based on an ontogenetic series of skeletal elements. J Vertebr Paleontol 20:115–129.

Hungerbühler A. 2002. The Late Triassic phytosaur *Mystriosuchus westphali*, with a revision of the genus. Palaeontology 45:377–418.

Hunt AP. 1989a. Cranial morphology and ecology among phytosaurs. In: Hunt AP, Lucas SG, editors. Dawn of the Age of Dinosaurs in the American Southwest. Albuquerue, New Mexico: New Mexico Museum of Natural History. p. 349–354.

Hunt AP. 1989b. A new ornithischian dinosaur from the Bull Canyon Formation (Upper Triassic) of east-central New Mexico. In: Hunt AP, Lucas SG, editors. Dawn of the Age of Dinosaurs in the American Southwest. Albuquerue, New Mexico: New Mexico Museum of Natural History. p. 355–358.

Jaekel O. 1910. Über einen neuen Belodonten aus dem Buntsandstein von Bernburg. Sitzungsber Ges Naturf Freunde Berlin 5: 197–229.

Klein N, Scheyer T, Tütken T. 2009. Skeletochronology and isotopic analysis of a captive individual of *Alligator mississippiensis* Daudin, 1802. Fossil Record 12:121–131.

Lamm E-T. 2013. Preparation and sectioning of specimens. In: Padian K, Lamm E-T, editors. Bone Histology of Fossil Tetrapods: Advancing Methods, Analysis, and Interpretation. Berkeley: University of California Press. p. 55–160.

Long RA, Ballew KL. 1985. Aetosaur dermal armor from the Late Triassic of southwestern North America, with special reference to material from the Chinle Formation of Petrified Forest National Park. Mus North Ariz Bull 47:45–68.

Lucas SG, Hunt AP, Spielmann JA. 2007. A new aetosaur from the Upper Triassic (Adamanian: Carnian) of Arizona. In: Lucas SG, Spielmann JA, editors. Triassic of the American West. New Mexico Mus Nat Hist Sci Bull 40:241–247.

Martz JW, Small BJ. 2006. *Tecovasaurus chatterjeei*, a new aetosaur (archosauria: stagonolepididae) from the Tecovas Formation (Carnian, Upper Triassic) of Texas. J Vertebr Paleontol 26:308–320.

Moss ML. 1969. Comparative histology of dermal sclerifications in reptiles. Acta Anat 73:510–533.

Nesbitt SJ. 2011. The early evolution of archosaurs: relationships and the origin of major clades. Bull Am Mus Nat Hist 352:292.

Parker WG. 2005. A new species of the Late Triassic aetosaur *Desmatosuchus* (Archosauria: Pseudosuchia). CR Palevol 4:327–340.

Parker WG. 2007. Reassessment of the aetosaur *'Desmatosuchus' chamaensis* with a reanalysis of the phylogeny of the Aetosauria (Archosauria: Pseudosuchia). J Syst Palaeontol 5:41–68.

Parker WG, Irmis RB. 2006. A new species of the Late Triassic phytosaur *Pseudopalatus* (Archosauria: Pseudosuchia) from Petrified Forest National Park, Arizona. Mus North Ariz Bull 62:126–143.

Parker WG, Martz JW. 2010. Using positional homology in aetosaur (Archosauria: Pseudosuchia) osteoderms to evaluate the taxonomic status of *Lucasuchus hunti*. J Vertebr Paleontol 30:1100–1108.

Parker WG, Martz JW. 2011. The Late Triassic (Norian) Adamanian–Revueltian tetrapod faunal transition in the Chinle Formation of Petrified Forest National Park, Arizona. Earth Environ Sci Trans R Soc Edinb 101:231–260.

Parker WG, Stocker MR, Irmis RB. 2008. A new desmatosuchine aetosaur (Archosauria: Suchia) from the Upper Triassic Tecovas Formation (Dockum Group) of Texas. J Vertebr Paleontol 28:692–701.

Parker WG, Irmis RB, Nesbitt SJ, Martz JW, Browne LS. 2005. The Late Triassic pseudosuchian *Revueltosaurus callenderi* and its implications for the diversity of early ornithischian dinosaurs. Proc R Soc Lond B 272:963–969.

Ponton F, Elzanowski A, Castanet J, Chinsamy A, de Margerie E, de Ricqlès A, Cubo J. 2004. Variation of the outer circumferential layer in the limb bones of birds. Acta Ornithol 39:21–24.

Reid REH. 1996. Bone histology of the Cleveland−Lloyd dinosaurs and of dinosaurs in general. Part I: Introduction to bone tissues. Brigham Young University Geology Studies 41: 25–72.

Ricqlès A de , Padian K, Horner JR. 2003. On the bone histology of some Triassic pseudosuchian archosaurs and related taxa. Ann Paleontol 89:67–101.

Romer AS. 1966. Vertebrate Paleontology. 3rd ed. Chicago: University of Chicago Press.

Rothschild BM, Schultze H-P, Pellegrini R. 2012. Herpetological Osteopathology. New York: Springer. 450 pp.

Salisbury SW, Frey E. 2001. A biomechanical transformation model for the evolution of semi-spheroidal articulations between adjoining vertebral bodies in crocodilians. In: Grigg GC, Seebacher F, Franklin CE, editors. Crocodilian Biology and Evolution. Chipping Norton, NSW: Surrey Beatty & Sons. p. 85–134.

Sire J-Y, Donoghue PCJ, Vickaryous M. 2009. Origin and evolution of the integumentary skeleton in non-tetrapod vertebrates. J Anat 214:409–440.

Scheyer TM, Desojo JB. 2011. Palaeohistology and external microanatomy of rauisuchian osteoderms (Archosauria: Pseudosuchia). Palaeontology 54:1289–1302.

Scheyer TM, Sander PM. 2004. Histology of ankylosaur osteoderms: implications for systematics and function. J Vertebr Paleontol 24: 874–893.

Schoch RR. 2007. Osteology of the small archosaur *Aetosaurus* from the Upper Triassic of Germany. N Jb Geol Palaeont Abh 246:1–35.

Schoch RR, Sues H-D. 2013. A new doswelliid archosauriform from the Middle Triassic of Germany. J Syst Palaeontol [doi: 10.1080/14772019.2013.781066].

Schwarz-Wings D, Frey E, Martin T. 2009. Reconstruction of the bracing system of the trunk and tail in hyposaurine dyrosaurids (Crocodylomorpha; Mesoeucrocodylia). J Vertebr Paleontol 29:453–472.

Stocker MR. 2010. A new taxon of phytosaur (Archosauria: Pseudosuchia) from the Late Triassic (Norian) Sonsela Member (Chinle Formation) in Arizona, and a critical re-evaluation of *Leptosuchus* Case 1922. Palaeontology 53:997–1022.

Stocker MR. 2012. A new phytosaur (Archosauriformes, Phytosauria) from the Lot's Wife beds (Sonsela Member) within the Chinle Formation (Upper Triassic) of Petrified Forest National Park, Arizona. J Vertebr Paleontol 32:573–586.

Stocker MR, Butler RJ. 2013. Phytosauria. In: Nesbitt SJ, Desojo JB, Irmis RB, editors. Anatomy, Phylogeny and Palaeobiology of Early Archosaurs and their Kin. Geol Soc Lond Spec Publ 379 [doi: 10.1144/SP379.5].

Sulej T. 2010. The skull of an early Late Triassic aetosaur and the evolution of the stagonolepidid archosaurian reptiles. Zool J Linn Soc 158:860–881.

Taborda JRA, Cerda IA, Desojo JB. 2013. Growth curve of *Aetosauroides scagliai* (Pseudosuchia: Aetosauria) inferred from osteoderm histology. In: Nesbitt SJ, Desojo JB, Irmis RB, editors. Anatomy, Phylogeny and Palaeobiology of Early Archosaurs and their Kin. Geol Soc Lond Spec Publ 379:413–4243 [doi:10.1144/SP379.19].

Trotteyn MJ, Martínez RN, Alcober OA. 2012. A new proterochampsid *Chanaresuchus ischigualastensis* (Diapsida, Archosauriformes) in the early Late Triassic Ischigualasto Formation, Argentina. J Vertebr Paleontol 32:485–489.

Vickaryous MK, Hall BK. 2008. Development of the dermal skeleton in *Alligator mississippiensis* (Archosauria, Crocodylia) with comments on the homology of osteoderms. J Morphol 269:398–422.

Vickaryous MK, Sire JY. 2009. The integumentary skeleton of tetrapods: origin, evolution, and development. J Anat 214:441–464.

Werning S, Irmis R, Smith N, Turner A, Padian K. 2011. Archosauromorph bone histology reveals early evolution of elevated growth and metabolic rates. J Vertebr Paleontol, SVP Program and Abstracts Book 2011:213.